Performance Evaluation of 5G Vehicle-to-Network Use Cases

A study of site configuration and network impact

Oskar Edwertz

Master's Thesis
Department of Electrical Engineering
Chalmers University of Technology
Gothenburg, 2017

Performance Evaluation of 5G Vehicle-to-Network Use Cases

O. Edwertz

The front page picture illustrates a three-sector base station deployed in a rural area. The image is provided and approved by Ericsson ©

Examiner: Henk Wymeersch
Supervisor: Tsao-Tsen Chen, *Ericsson*
Adviser: Markus Fröhle, *Chalmers*

Chalmers University of Technology
Department of Electrical Engineering
SE-412 96 Gothenburg
Sweden
Telephone + 46 (0)31-772 1000
Gothenburg, Sweden October 2017

Abstract

The automotive sector is rapidly becoming more connected, which imposes many new challenges. A possible solution for the yet to be decided wireless network is to use cellular vehicle-to-network (V2N) communication. This thesis showcases a performance evaluation for three different use cases in an automotive scenario: mobile broadband (MBB), transmission of high definition maps (HDM) and remote driving (RD). Both LTE (Long-Term Evolution) and 5G new radio (NR) are considered in this thesis, and simulated using a large set of different configuration setups. Requirements and traffic demands are derived for each use case and a method for generating road maps based on real data is presented. The key takeaway is that the MBB traffic is heavily impacted by the investigated V2N use cases. It is shown that in order to meet the 2022 MBB requirement it is a necessity to use carrier aggregation (CA), where an aggregated 40 MHz bandwidth (BW) is able to fulfill the demand under the assumed network scenario. Furthermore, it is demonstrated that the HDM requirement is satisfied when either relying on a 5G NR standalone 100 Mhz BW setup, deployed on a dedicated V2N carrier, or a LTE-NR 120 Mhz BW interworking solution. Lastly, it is indicated that the RD use case is a great challenge, and none of the setups in this thesis were able to fulfill the requirement for the worst-case traffic scenario. In order to satisfy this use case solutions such as multi-user multiple-input multiple-output (MIMO), larger BW and a denser network deployment are proposed.

Keywords: Network performance, V2N, LTE, 5G, remote driving, high definition maps

Acknowledgement

First and foremost I want to express my kindest thanks to my supervisor Tsao-Tsen Chen. A more patient and pedagogic person is hard to find. Thank you for everything you have taught me and for providing your full support throughout the thesis.

I also want to show my gratitude to Dirk Gerstenberger. Thank you for giving me the opportunity to conduct this thesis at Ericsson and thank you for the kindness you have shown me.

A big thank you to my examiner Henk Wymeersch for allowing me to commence this thesis, and for the inspiring teaching at Chalmers. Next in order I want to thank my adviser Markus Fröhle for giving me great guidance and technical feedback from start to finish.

I am giving a whole-hearted thank you to my best, life-long friend, Klas Tauberman. No words can describe how grateful I am for you. Your everlasting support and friendship mean the world to me.

I wish to thank my beloved family for their encouragement and their fantastic ways of bringing joy to life, which have made my educational journey great. Mom and Dad you are the best parents anyone could ask for, I love you with all my heart.

Lastly I want to acknowledge the hard working community of OpenStreetMap.
Map data copyrighted OpenStreetMap contributors and available from https://www.openstreetmap.org

Contents

Acronyms

5GAA 5G Automotive Association. 1

AOSA array of sub arrays. 5, 7, 23

BS base station. 5, 6, 7, 13, 14, 20, 21

BW bandwidth. 2, 42

CA carrier aggregation. 2, 7, 8, 24, 25, 43

CC component carriers. 7, 8

C-V2X cellular-vehicle-to-everything. 1

DC dual connectivity. 8, 9, 43

DL downlink. 2, 6, 12, 13, 15, 23, 24, 25, 27, 33, 38

FSPL free-space path loss. 5

HDM real-time high definition maps. 1, 2, 11, 14, 20, 23, 27, 32, 38, 42

ISD inter-site distance. 2, 13, 20, 21, 43

ITS intelligent transportation systems. 1

LDM Local Dynamic Maps. 2

LoA level of automation. 10

MBB mobile broadband. 1, 2, 11, 12, 20, 23, 42

MIMO multiple-input multiple-output. 5, 6, 42, 43

MRC maximal-ratio combining. 7

NR new radio. 1, 2, 8, 23, 25

OSM OpenStreetMap. 2, 15, 16, 17

RD remote driving. 1, 2, 11, 20, 23, 32, 38, 42

SA sub arrays. 5, 6, 7, 23, 26

SNR signal-to-noise ratio. 7

UE user equipment. 1, 5, 6, 8, 12, 20, 23

UL uplink. 2, 6, 8, 12, 13, 15, 23, 24, 25, 32, 38, 41

V2I vehicle-to-infrastructure. 2

V2N vehicle-to-network. 1, 2, 23, 24, 25, 38, 42, 43

V2X vehicle-to-everything. 2

1 Introduction

With the present-day swift evolution in both the communication sector and the car industry, new standards, technologies and partnerships are bound to happen. As the modern car fleet is becoming both more connected and more autonomous, the cellular network load is expected to increase, especially in rural areas where the site deployment is more sparse. However, before going into detail and depth regarding the findings and conclusions of the thesis, it is first of essential to provide a brief introduction. This chapter provides a background survey, project description, scope, related works, as well as a thesis outline. Presenting this kind of project overview serves to facilitate the understanding of the more technical sections presented later on. As made clear in this chapter, the research area of the thesis is both new and prominent.

1.1 Background

While much of the data required to establish self-driving cars can be transferred using short-distance communication, many scenarios depend on information that is not obtainable from within a close proximity. For these longer communication paths, the cellular network could be a potential solution for communication both between vehicles and to the network itself, so called vehicle-to-network (V2N) communication. A couple of possible use cases could for example be: warning indications for obstacles or traffic congestion far ahead, a centralized positioning system, remote controlling of vehicles, sending and downloading detailed sensor data (dynamic maps), as well as vehicle status/health reports. Many of these use cases are highly probable of becoming realized, for instance, the 3GPP release 14 includes initial services and use cases for cellular-vehicle-to-everything (C-V2X) communication. Furthermore, the 5G Automotive Association (5GAA) is a collaboration between a large set of industries with the ambition of accelerating the establishment of autonomous vehicles and intelligent transportation systems (ITS). Lastly, it is worth mentioning that various applications have already been realized by the industry, such as real-time high definition maps (HDM) [1].

The next generation of mobile networks will be launched in the near future, enabling vast improvements on nearly all system performance metrics. One important factor is the big leap of the user capacity, which will enable the network to handle a larger set of user equipment (UE) simultaneously. This is essential, as the vehicle connectivity is bound to see a great expansion. However, standards for the 5G network have not yet been completely decided upon, making accurate simulations profoundly difficult. At the same time, the mobile broadband (MBB) traffic per user is expected to grow exponentially over the next few years [2], putting high pressure on the coverage demands. At Ericsson, most network deployment studies so far have focused on MBB, rather than automotive deployments, which is one of the key motivations behind this thesis. To further expand on the fundamental ambition of the project the next subsection goes into detail regarding both the general description, as well as the purpose of the thesis.

1.2 Problem Definition

The main purpose of the thesis is to create a simulation program that can be used for different automotive scenarios, where one of the main catalysts is that these kinds of vehicle simulations are a rather unexplored area for the company. After constructing a motorway scenario, the study will be surrounding the topics of automotive radio network deployment. Hence, the purpose can be summarized as finding deployment scenarios which will fulfill the estimated traffic and throughput requirements. By doing so, it will become evident to what extent LTE and 5G new radio (NR) are able to perform in these selected operations (use cases).

There are many potential use cases to investigate. However, simulation of MBB, HDM and remote driving (RD) are the ones that will be considered in this thesis, which will be further explained in section 1.3. In conclusion, the thesis aims to showcase a performance evaluation of a set of 5G use cases, where different deployments will be simulated and the traffic impact of the mentioned operations will be shown.

To make the problem description more clear, a couple of key questions are here presented. The objective is considered to be fulfilled once these questions are answered and have all been thoroughly processed.

- What network requirements can be expected from the three use cases?
- Can these requirements be fulfilled when using standardized LTE technology?
  - What is the impact on MBB when adding the other use cases?
  - How does carrier aggregation (CA) improve the results?
  - What inter-site distance (ISD) is suggested in order to meet the traffic demand and user throughput requirements?
- Is NR technology able to boost the performance of the LTE case?
  - What performance gain is achieved when combining LTE and NR technology?
  - What antenna configuration should be used in order to achieve the best performance?
- Is the map generation code adaptable for future use and new scenario configurations, such as new use cases?

1.3 Scope

An important factor to consider when ensuring that the outcome of the thesis will be of high quality, is the scope. The topic of this thesis is very broad, and is therefore subject to a lot of research possibilities. Because of this, it is especially important to narrow down the focus points and set a reasonable scope. As mentioned before, the thesis is limited to only consider three different use cases: MBB, HDM and RD. The first of the three simply implies that the user traffic from within the cars is considered. The second use case concerns the sensor data gathered by the vehicles in order to build a robust navigation system and the third and last use case is about taking control of a car remotely. The same propagation channel is used for all three use cases, which is further explained in section 2.1. Since there are many different use cases that could be evaluated, it is essential to create a program that can be used for future work. The thesis will only consider V2N communication, and not the more general vehicle-to-everything (V2X). Furthermore, for each of the use cases both downlink (DL) and uplink (UL) transmission will be taken into consideration. The thesis is evaluating both LTE and NR performance, and investigates the impact of CA between both LTE bands and LTE and NR bands (interworking). The thesis is limited to only aggregate two bands, and only the low to mid frequency spectrum is considered. Due to this, CA between two NR bands is not studied in this work.

1.4 Related Works

While there are many papers discussing V2X communication using 5G technology, few go into detail regarding network performance and deployment scenarios. The 5G Infrastructure Public Private Partnership (5G-ppp) thoroughly talks about the future of automotive use cases and their potential use of 5G in a published white paper [3]. A few interesting points are made, such as the limitations of the current communication systems when handling the assumed vehicular communication. For instance, as the current 3GPP system is designed for serving MBB traffic, implementing short V2X messages may cause a great waste of resources[3].

Furthermore, [4] provides useful requirement predictions on a large set of automotive use cases. For instance, data is presented for the remote controlled car use case, as well as numerical data for a use case scenario called "sensor and state map sharing", which is quite similar to the one concerning transmission of HDM. However, as their interpretation appears to be more extensive than the use case presented in this thesis, their potential requirements are not included in this work.

According to [5], it is investigated how the latency of Local Dynamic Maps (LDM) is increased when the number of vehicles is growing. The paper shares some relation with this thesis, not only because they construct a vehicle road map from real data using OpenStreetMap (OSM), but also because HDM can be seen as a part/layer of LDM. However, as already mentioned their paper focuses on the latency concerns of the database management system and does not consider any wireless network during their implementation.

Another paper [6] studies the network performance for vehicle-to-infrastructure (V2I) communication when having real-time critical applications in mind, which can be compared with the HDM use case in this thesis. The simulation scenario is quite similar, but their V2I setup does not share the same spectrum as the MBB users. Other differences are for instance; they look at a highway scenario with six lanes instead of four, they only consider one velocity (v = 140 km/h), they only simulate DL communication, they have their bandwidth (BW) fixed at 10 Mhz, and they use a stricter reliability criterion in comparison to the HDM messages (99.999 % vs 95%). The last-mentioned difference comes from the V2X reliability requirement derived from the METIS 2020 Project [7], but newer reports from 3GPP show more relaxed reliability values for a large set of V2X applications [4]. Furthermore, the paper only investigates standalone LTE, neither CA nor NR technology is considered. The paper concludes that new resource allocation is needed if strict reliability V2I communication should be fully supported.

The article [8], compares 802.11p and the vehicle modified architecture LTE-V, which is based on TD-LTE. The proposed LTE-V technology is operated over two different modes; LTE-V-Cell (V2N and V2I) and LTE-V-Direct (V2V). However, only the LTE-V-Direct mode is simulated. The article shares some relation with this thesis as they have also proposed a model for an automotive scenario. An interesting way of mapping the highway model to a city model is showcased.

Lastly, another related work is a master's thesis conducted at Ericsson [9]. The thesis evaluates many different system metrics and investigates the network performance for Air-to-Ground communication using 5G technology. While the study handles different simulations, some similarities to the methodology can be noticed. For instance, the generation of the network map, as well as the analysis of the NR array configuration.

1.5 Thesis Outline

In order to give the reader a better understanding about the surroundings of the thesis work, purpose and scope, the report starts with a brief introduction and related works, as shown above. This is followed by a chapter entirely dedicated to theory, which strives to give the reader the necessary components to better grasp the underlying concepts and techniques used throughout the thesis. Worth mentioning is that even though not all of the theory subjects are directly processed by the thesis work itself, it is still vital to introduce the reader to these areas, in order to get a bigger picture, and understand studies in related fields.

After have being introduced to the theory, the reader will shift his attention to the method of the work, which is where the different use cases are explained in more detail. Here the reader will find the necessary estimations and predictions, as well as the defined requirements for each of the use cases. The thesis will then go into detail regarding the setup of the simulations, before showcasing the results. Lastly, the report concludes with a conclusion of the thesis findings and a chapter explaining what can be improved or further investigated in potential future work.

2 Theory

In this section a few integral concepts are introduced. First off, general propagation theory is highlighted, while at the same time presenting areas more closely connected to this thesis, such as array configuration and statistical models. Later on, carrier aggregation is explained, which is an essential element of the thesis. Lastly the more general topics of vehicular safety and next generation networks are presented.

2.1 Propagation Model

Different propagation models should be applied for different scenarios. For the case of this thesis, which concerns rural areas, content from the ITU RMa model is partly implemented [10]. While the complete propagation model technicalities are not showcased in this thesis, some brief details can be seen in section 2.1.4.

2.1.1 Free Space Path Loss

The free-space path loss (FSPL) equation describes the power attenuation of a signal with frequency f when traveling over a distance d. The formula assumes line-of-sight transmission in free space with isotropic antennas, and is derived from the inverse of Friis transmission equation [11], which describes the power gain between receiving and transmitting antennas. Friis formula is expressed as,

$$\frac{P_r}{P_t} = D_t D_r \Big(\frac{\lambda}{4\pi \cdot d}\Big)^2, \tag{1}$$

where P_r and P_t are representing the power at the receiving and transmitting antennas respectively. The variables D_r and D_t correspond to the isotropic directivity of the antennas. Hence, when expressing FSPL, equation 1 is inversed and $D_r = D_t = 1$. Thus,

$$\text{FSPL} = \Big(\frac{4\pi \cdot d \cdot f}{c}\Big)^2, \tag{2}$$

where λ has been replaced with c/f. The equation is often described in decibel scale according to,

$$\text{FSPL} = 20 \cdot \log(d) + 20 \cdot \log\Big(\frac{4\pi}{c}\Big) + 20 \cdot \log(f). \tag{3}$$

The resulting equation can be seen as a lower bound to the actual path loss, for which more fine-tuned formulas are needed.

2.1.2 Antenna Gain

Antenna gain is defined as the experienced gain when transmitting or receiving in the same direction as the main lobe of the antenna. As previously mentioned, the FSPL equation assumes isotropic antennas, which normally is not the case. Despite of this, the UEs are considered isotropic in this thesis, but the base station (BS) antennas are not. Instead, they have an antenna gain dependant on the location of the UE, meaning that the gain varies over an interval, as will be shown in the next subsection.

2.1.3 Antenna Array Configuration

With the advancement to new exceedingly higher frequencies comes the benefit of smaller antenna elements, as the antenna size is growing inversely proportional to f [12]. This allows for Massive multiple-input multiple-output (MIMO) systems and advanced beamforming techniques, as a larger number of antenna elements can fit in a relative small area. In this fashion, the energy is focused into a smaller volume of space, yielding both a higher spectral efficiency and throughput. The antenna array configuration can be realized as the combination of sub arrays (SA) and an array of sub arrays (AOSA), which is depicted in figure 1. Studies have shown that systems using the same number of antenna elements, but with different array layouts may achieve completely different performance depending on the deployment scenario. Furthermore, antenna arrays hosting a large set of elements are tremendously expensive, as each of the digitized antenna elements requires its own radio chain. Hence, for large arrays it is common to use a hybrid solution, where only a selection of the elements are digital and the rest are instead analog (one common radio chain).

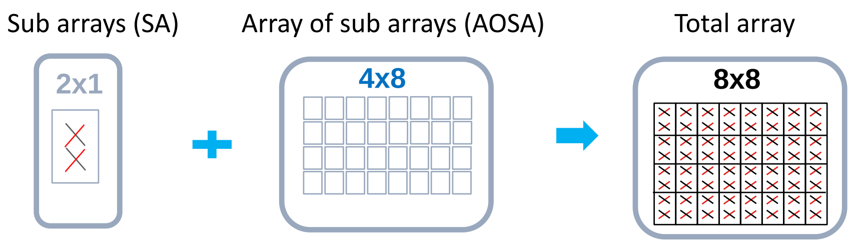

Figure 1: Showing how the total array can be represented by the sum of sub arrays and an array of sub arrays

For this thesis, each SA consists of a number of dual-polarized elements and generates two concurrent signal streams, one per elements with the same polarization. A large number of different configurations are experimented with, a few of which can be seen in figure 2.

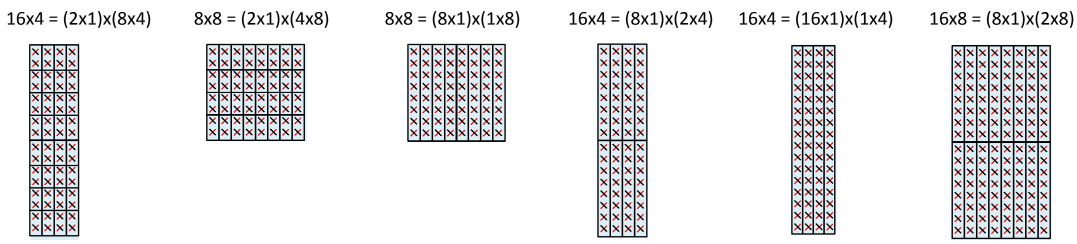

Figure 2: Showcasing a couple of different array configuraitons

The massive MIMO system provides both diversity and multiplexing gain, where the foremost retaliates the effect of deep fading and hence improves the transmission reliability, and the latter improves the system throughput. In order to ensure that the fading channels are decorrelated, the antennas need to be placed sufficiently far apart from each other. Another way of achieving array gain is to place the antennas closely together and instead rely on beamforming techniques. This is done in the DL, where different weights are put on each antenna in order to create a narrow and focused beam. The BS antenna gain consists of three parts: the element gain, the SA gain and the array gain. In this thesis the element gain at the BS is around 6.5 dBi, for both DL and UL. The SA, which also is accounted for in DL and UL, depends on the SA size and the UE location. The maximum SA gain G_{SA} is computed as,

$$G_{SA} = 10 \cdot \log_{10}(S1), \tag{4}$$

where S1 is the size of the SA. For example, using the SA seen in figure 1, the maximal SA gain is $10 \cdot \log_{10}(2) = 3$ dB. The beamforming technique applied in this thesis provides a DL array gain dependant on the UE location, as well as a channel co-variance matrix. The maximal array gain G_A is computed according to,

$$G_A = 10 \cdot \log_{10}(S), \tag{5}$$

where S is the total size of the AOSA. For example, using the AOSA seen in figure 1, the maximal array gain is equal to,

$$G_A = 10 \cdot \log_{10}(4 \cdot 8) = 15 \text{ dB}. \tag{6}$$

Furthermore, at the receiving side of the system a diversity combining technique is implemented. A common technique is maximal-ratio combining (MRC), which simply puts weights on every received signal depending on its signal-to-noise ratio (SNR). The accumulated SNR is thus calculated as,

$$\sum_{k=1}^{S} \mathrm{SNR}_k \tag{7}$$

where k indicates the index of the received signal. This means in theory that a 3dB gain can be expected per added signal, which is not the case in practice. For the simulations in this thesis a constant gain of 2.5dB is added per doubling of S. Hence, the gain achieved from MRC is only depending on the array size, and not the configuration. For instance, by using the same example as above, the MRC gain is calculated as,

$$G_{\mathrm{MRC}} = 2.5 \cdot \log_2(4 \cdot 8) = 12.5 \text{ dB}. \tag{8}$$

Note that the array gain in DL and the MRC gain in UL are on top of the element gain and SA gain. That is, the total DL BS antenna gain is equal to element gain + SA gain + array gain, while the total UL BS antenna gain is equal to element gain + SA gain + MRC gain.

2.1.4 Statistical models

The propagation model used for this thesis is a statistical one, mainly because no building data is used for the highway scenario (which limits the use of site-specific models). In this case, a statistical model implies an estimated path loss, log-normal distributed shadow fading, as well as an average car penetration loss, among other parameters. Multi-path fading, which normally is modelled using a Rayleigh distribution [13], is not considered in this thesis due to the time-independent property of the simulator. The effect is however accounted for by other means.

The path loss is derived using a large set of different methods and techniques. For instance, Okumuras-Hata's wave propagation equations are used with some adjustment, attenuation by communication between far apart receiver/transmitter, as well as wave propagation loss caused by various disturbances [14] [15].

2.2 Carrier Aggregation

With the launch of LTE-Advanced (release 10), a technique called carrier aggregation (CA) was introduced. The idea is simple, by aggregating a collection of carriers, known as component carriers (CC), the data rate and capacity are vastly increased and fragmented spectrum can be put to use. With a maximum of five CCs and 20 Mhz per carrier, a total of 100 MHz may be aggregated [16]. There are three different ways to aggregate these components.

- Intra-band contiguous

- Intra-band non-contiguous
- Inter-band

The first of the three implies that all the CCs are within the same frequency band and the aggregated carriers are next to each other in frequency. By inspecting figure 3, a clear example of intra-band contiguous CA, would be to combine CC_1 and CC_2. The next method is intra-band non-contiguous, and as the name suggests, this means that the CCs are located in the same frequency band, but are not adjacent to each other. An example of this would be to aggregate CC_1 and CC_3 in figure 3. The last technique is inter-band CA, where CCs from different frequency bands are combined. By inspecting the same figure, an example would be to aggregate CC_3 and CC_4.

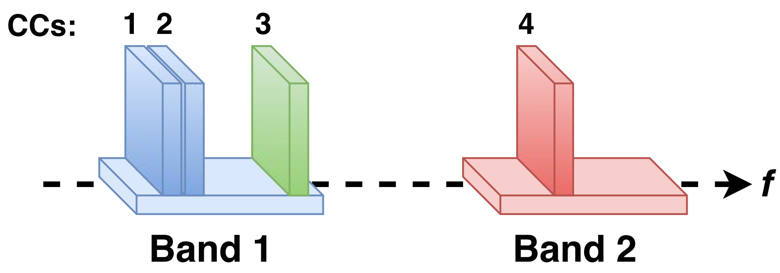

Figure 3: Two different frequency bands together with four component carriers

In this thesis, CA is regularly used in the simulations, as shown explicitly in section 4. While the technique can be used in the uplink, this is not always the case. By simulating CA in the UL and giving the same maximum UE output power for each band, it is assumed that the UE can produce a vast increase of output power. For example, if two frequency bands are aggregated, the maximum output power (23 dBm) needs to be doubled and transmitted over both bands separately, which represents a best-case performance scenario with a linear improvement in respect to added CCs. Figure 4a illustrates this best-performing scenario, while figure 4b and 4c instead showcase the worst-case scenario where an an increase in maximum output power is not possible. It should be noted that the output power is actually not necessarily divided evenly across the bands, as seen in the previously mentioned figures, but instead can be allocated unevenly across the bands to optimize the overall performance.

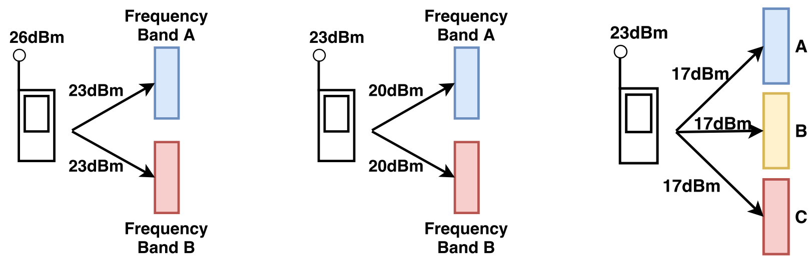

(a) (b) (c)

Figure 4: (a) Best-case scenario: The UE maximum output power is doubled, since maximum 23 dBm can be transmitted per frequency band (A and B). (b) Worst-case scenario: The UE maximum output power remains the same and the transmit power per frequency band is split in two. (c) Worst-case scenario: In similar fashion, the power is slit in three when having three CCs

As an increasement of maximum output power on this order is not possible for a normal UE, due to maximum emission regulations [17], the simulations showcasing CA in the UL should instead be seen as an upper-bound. A more common UL technique is instead band selection. This method scans the available frequency bands and transmit on the one with the best performance. This implies that the UL transmission would be limited to a one single band. In terms of performance, choosing the frequency band by using band selection shows an improvement in comparison to relying on a pre-selected frequency band.

Lastly, when it comes to 5G and the planned features in the upcoming releases, there are yet no concrete plans of including support for CA interworking (i.e. one LTE carrier and one NR carrier). Instead, LTE-NR dual connectivity (DC), is expected to become the state-of-the-art interworking technology. The DC model implies that a user can simultaneously be connected to multiple bands transmitted from cells in the same site or different sites. A user may therefore receive data from two aggregated bands, sent from different sites, thus mimicking the technique of inter-site CA [18]. However, as an ideal interface, like fiber, between the sites is not always available, the near linear performance boost from CA is most certainly not achievable when using DC. Instead, when compared to inter-site CA with ideal interface between sites, there will be some performance loss for inter-site DC due to the use of non-ideal interface (for example, X2 interface) between the sites.

The choice of using cross-technology CA in this thesis despite the lack of implementation details is motivated by the following points:

- DC models are not supported in the simulator tool
- The cross-technology CA model provides a best-case approximation for LTE-NR DC interworking (ideal backhaul, such as fiber)
- It is probable that cross-technology CA will be considered in a future release

2.3 The Fifth Generation Network

The next generation of cellular communication (5G) aims to advance the current technology capabilities by achieving both vastly higher throughput and capacity, while also providing promise of sub-1ms latency. These enhancements open up for not before achievable applications and use cases. It is essential to have in mind that a 5G network is not a technology, but rather an unification of technologies. A 5G network will largely rely on the LTE evolution technology, which continues to be the main focus point in on-going development [19]. At the same time new radio technology is being considered together with millimeter wave spectrum. As is showcased in figure 5, 5G acts as the bigger picture and consolidates these technologies and spectrum by implementing tight interworking methods.

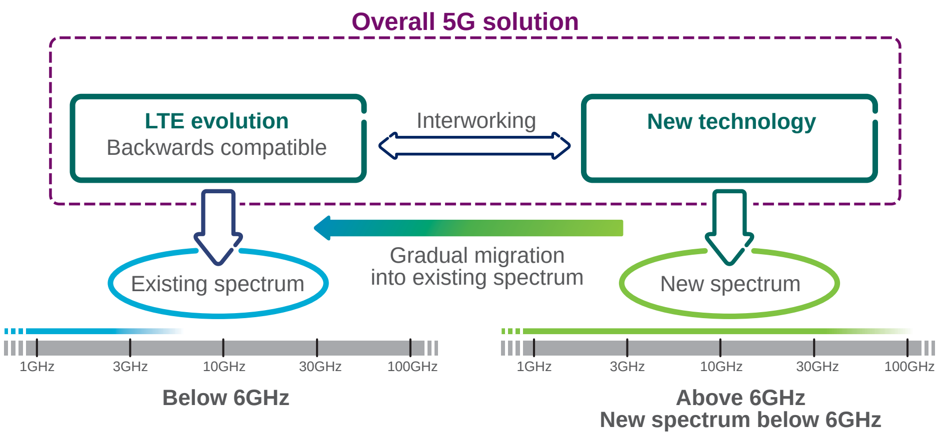

Figure 5: Overview of the 5G deployment. The figure is gathered from a white paper published by Ericsson [20]

As previously mentioned, 5G opens up for new technology concepts and improvements. For instance, device-to-device (D2D) communication, massive MIMO and dynamic time division duplex (TDD) [20]. When it comes to the latter, it is fundamental to know that 5G networks will continue to use FDD as the main duplex technique for low frequencies. However, for higher frequencies TDD may be favourable. Not only does this enable reciprocity based beamforming, where the same channel estimation can be used for DL and UL, but also it allows for an adaptable and more efficient transmission scheme. This is considered to be vital for the small-cell dense deployments, as the traffic demands will be very fluctuating in these cells. Hence, by combating this with a rapid and flexible TDD ratio technique, the spectrum will be used more efficiently. This kind of flexibility is also supported with current LTE technology to some extent, such as with TD-LTE. However, due to restrictions on DL/UL configurations the dynamic aspect is lost in practice [20]. With the 5G network it is aimed to relax these restrictions and with it allow a more efficient system.

2.4 Vehicle Safety and Communication

Ever since the 1970s the number of fatalities due to car accidents has seen a declining trend, despite the linear increase of vehicle traffic [21]. Over these years new technologies have made vast improvements on vehicle safety. The technologies range from more passive, such as seat belts and airbags, to more active, such as ABS and lane assisting systems. The next technical breakthrough in vehicle safety is beyond any doubt the advancement of vehicle connectivity and communication. The enabling of vehicle communication improves not only safety aspects, but also environment prospects through enhancement of traffic efficiency. Furthermore, the expansion of this communication acts as a vital ingredient to achieve fully autonomous cars.

Bringing out a fully autonomous car has for the past few years become both a pressing and prestigious objective for many car manufacturers, which has resulted in an acceleration in research and development. In order to categorize the vehicles based on their current capabilities the term level of automation (LoA) has been defined. These different levels, ranging from zero to five, are well explained in table 1. Analyzing this table may help when setting guidelines for future use cases and expected network load.

Table 1: The different levels of automation explained. The table is produced by SAE International and contained in standard J3016 [22]

SAE level	Name	Narrative Definition	Execution of Steering and Acceleration/ Deceleration	*Monitoring* of Driving Environment	Fallback Performance of *Dynamic Driving Task*	System Capability *(Driving Modes)*
***Human driver* monitors the driving environment**						
0	No Automation	the full-time performance by the *human driver* of all aspects of the *dynamic driving task*, even when enhanced by warning or intervention systems	Human driver	Human driver	Human driver	n/a
1	Driver Assistance	the *driving mode*-specific execution by a driver assistance system of either steering or acceleration/deceleration using information about the driving environment and with the expectation that the *human driver* perform all remaining aspects of the *dynamic driving task*	Human driver and system	Human driver	Human driver	Some driving modes
2	Partial Automation	the *driving mode*-specific execution by one or more driver assistance systems of both steering and acceleration/ deceleration using information about the driving environment and with the expectation that the *human driver* perform all remaining aspects of the *dynamic driving task*	**System**	Human driver	Human driver	Some driving modes
***Automated driving system* ("system") monitors the driving environment**						
3	Conditional Automation	the *driving mode*-specific performance by an *automated driving system* of all aspects of the dynamic driving task with the expectation that the *human driver* will respond appropriately to a *request to intervene*	System	**System**	Human driver	Some driving modes
4	High Automation	the *driving mode*-specific performance by an automated driving system of all aspects of the *dynamic driving task*, even if a *human driver* does not respond appropriately to a *request to intervene*	System	System	**System**	Some driving modes
5	Full Automation	the full-time performance by an *automated driving system* of all aspects of the *dynamic driving task* under all roadway and environmental conditions that can be managed by a *human driver*	System	System	System	**All driving modes**

3 Method

In this chapter the methodology of the thesis is presented. First off, the use cases are further explained, highlighting the needed estimations in order to reach the defined requirements. Thereafter, the simulation scenario is showcased in form of describing the process of map and network generation, as well as the simulation parameters.

3.1 Use Cases

As previously mentioned in Section 1, the thesis involves three different use cases, which are in this section explained in greater detail. In addition to this, the traffic requirements, as well as the needed estimations for each use case are presented.

In order to get a general picture of the simulation outline it is of essence to recognize that the three use cases are closely connected and can be seen as a gradually increase of car connectivity. While the simulation can be done for a combination of the use cases, the car pattern remains the same, meaning that the overall car density is independent of the selected use case. Instead, this parameter depends on the velocity of the cars.

By assuming a constant flow of cars on the motorway, which means that the cars have a fixed distance between each other, it is possible to estimate the car density. Each car occupies an area equal to $lane\ width \cdot (car\ length + safety\ distance)$, where both the lane width and the car length are set to 4 m. The safety distance is defined based on the expected reaction time, as well as the vehicle velocity. The reaction time is set to 1.8 seconds [3], and the velocity v is selected as 24, 70 or 140 km/h. Hence, the area A per car is expressed as

$$A = 4 \cdot (4 + \frac{v}{3.6} \cdot 1.8). \tag{9}$$

For a velocity of 24 km/h this yields a car area of 64 m^2, for 70 km/h an area of 156 m^2, and for 140 km/h an area of 296 m^2. The respective car densities are thus 15625, 6410 and 3378 cars per km^2, where only the motorway area is considered. Figure 6 illustrates the occupation area for a car when the vehicle flow is set to 24 km/h. For the cars outside the motorway the velocity-density correlation is disconnected, and a static value of 100 cars per km^2 is used, which is reasonable for a rural area. The cars outside the motorway are purely there to generate background noise, and since the study is mainly about motorway traffic, it is justified to set this parameter to static.

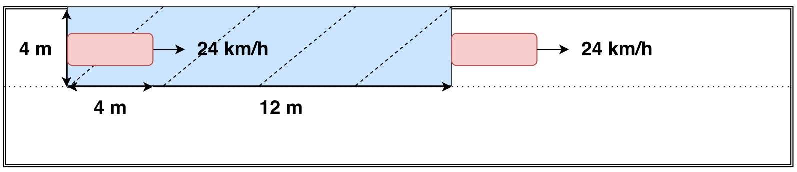

Figure 6: The dashed rectangle represents the area occupied by one car. In this example the cars are moving with a velocity of 24 km/h, which gives an area of 64 m^2. For simplification reasons only cars on one lane are shown.

The data traffic from each individual car depends on which use cases are active for this specific car. For instance, one car can transmit and receive data for MBB, HDM and RD at the same time, as is presented in Figure 7. However, when investigating the impact of one particular use case, it might be of interest to limit this variability. It is also worth mentioning that in the current simulation build each of the use cases is impacted by the same vehicle penetration loss. Making this parameter variable as well should be considered during potential future work, see section 6 for more details. Furthermore, by knowing the motorway area of the region of interest, it is easy to calculate an expected quantity of cars occupying the road. The total highway area for the considered location is 371264 m^2, hence the expected number of cars on the highway is 5801, 2380 and 1254 for a velocity of 24, 70 and 140 km/h respectively. These numbers can be converted to cars/km, which gives 25, 10 and 5 cars/km for each velocity separately. In addition to this, by using the occurrence data from section 3.1.2 and 3.1.3, it is also possible to calculate the number of HDM and RD cars per km. These values are captured in table 2. By taking the velocity $v = 140$ km/h as an example, it is seen that one HDM car every 2 km and one RD car every 200 km is expected.

Table 2: Number of HDM and RD cars per km for each velocity

	24 km/h	70 km/h	140 km/h
HDM cars per km	2.5	1	0.5
RD cars per km	0.025	0.01	0.005

Each of the use cases has its own traffic demand and requirements, defined separately for the DL and UL. These parameters need to be estimated as accurately as possible, in order to better represent the real world. This is the main content of the following subsections, which start with the simplest of the three applications, MBB.

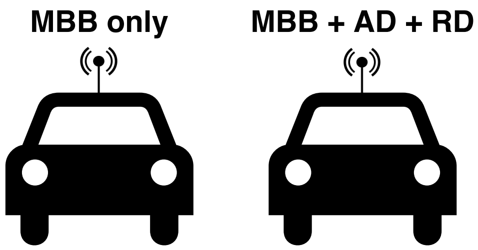

Figure 7: A car may be equipped with both AD and RD capabilities, while simultaneously having connected MBB users inside the car.

3.1.1 Mobile Broadband

In layman's terms, mobile broadband simply implies data generated by an UE, which often are hand-held devices, such as mobile phones. Studies on MBB have been widely covered by Ericsson, and predictions on future data consumption in terms of GB/User/Month can be found in their latest mobility report [2]. According to this report it is expected that an average user consumes 22 GB of data per month in western Europe by year 2022. This data is divided between the DL and UL as 90 % and 10 % respectively.

As a car may contain multiple people, it cannot be considered as one UE itself. Therefore, a necessary aspect to explore is how many MBB users on average are expected in one car. According to the European Environment Agency the average number of people in a passenger car is 1.45 [23], however, the driver is probably not consuming as much data as the passengers in the car. This is why the data generated by the driver is approximated to be 50% less than a normal MBB user. By using this assumption the number of MBB users per car is presented as $1.45 - 0.5 = 0.95$.

In combination with the derived consumption number, internal Ericsson reports indicate a throughput requirement of 10 Mbps and 1 Mbps for the DL and UL respectively, as well as a transmission reliability of 95%, which is illustrated in table 3.

Table 3: Summary of the requirements for the mobile broadband use case

Traffic demand	22 GB/User/Month
Downlink	10 Mbps
Uplink	1 Mbps
Reliability	95 %

3.1.2 Real-time High Definition Maps

This use case is about the transmission of high definition road maps, which are used to both map the road, and to provide a very accurate localization technique for the vehicle. It is assumed that autonomous cars use these maps, as the accuracy of a GPS system is not precise enough. The road map is gathered from installed in-vehicle equipment and the data is processed inside the car before being sent in UL. The uploaded data is stored in the cloud, where it is accumulated with the data from other cars. A more accurate map can then be sent back to the vehicles in the region.

The size of the high definition maps greatly depends on the technology used. According to Mobileye, recently acquired by Intel, their camera technology sensors transmit as low as 10 kB/km [24]. On the other hand, maps generated using 3D laser technology may require as much as 10 MB/mile $\approx$ 6 MB/km when using lossless compression [25]. It is yet to be decided by the industry which technology will be considered state-of-the-art. Hence, in order to capture a wider set of future possibilities, three different sizes are investigated in this thesis; 10 kB/km, 2 MB/km and 4 MB/km. In the next estimations it is assumed that one transmission is sent every km in the UL, and that the vehicles travel by a speed of 24, 70 or 140 km/h. By using these values we calculate the time interval t per data transmission according to

$$t = \frac{1000}{\frac{v}{3.6}}. \tag{10}$$

Hence we have 1 message every t seconds, which also equals to 1/t messages per second. The data traffic D in the UL can therefore be expressed as,

$$D_{UL} = d \cdot \frac{1}{t} \cdot 8 \text{ bps}, \tag{11}$$

where d is the data size of the high definition map. By inserting the different values for v and letting $d = $ 10kB/km, the data traffic in UL is approximated to 0.53, 1.55 and 3.11 kbps/car for the respective velocities.

When estimating the data traffic in the DL more assumptions are needed:

- Unicast transmission mode
- The BS is placed very close to the highway, which normally is the case for remotely located roads. An example of this can be seen in figure 8
- The highway got two lanes per direction
- The vehicle speed is 24, 70 or 140 km/h
- The ISD, which simply means the distance between two BS, is selected to be 2 km
- The length of the cars is 4 meters
- The reaction time of the driver is 1.8 seconds [3]
- The probability p of having a car with HD map gathering capability in 2022 is predicted to be 1%, which is based on the hypothesis of 10 million semi-autonomous cars by 2020 [26]

and the current car fleet size. In order to look further into the future, this percentage is also experimentally selected as 10 %

Using these assumptions we get that,

$$D_{DL} \approx D_{UL} \cdot \lceil N \rceil \,, \tag{12}$$

where N is the number of cars served by one cell in the DL,

$$N = \frac{4 \cdot p \cdot 2000}{4 + \frac{v}{3.6} \cdot 1.8} \cdot \frac{1}{3}, \tag{13}$$

and where the divisor 3 comes from the fact that each BS is divided into three cells. The resulting DL data traffic is shown in table 4. As can be seen, the bit rate decreases when the vehicle speed is increased, since the safety distance grows, while it increases when the density of semi-autonomous cars also increases.

Table 4: Data traffic per car in DL when considering transmission of high-definition road maps. When the velocity increases the data per car goes up, but at the same time fewer cars will be served, due to a larger safety distance. All numbers are in kbps

Map size 10 kB/km		
Speed \ Density	1%	10%
24 km/h	0.53	8.53
70 km/h	1.56	9.33
140 km/h	3.11	9.33

Map size 2 MB/km		
Speed \ Density	1%	10%
24 km/h	106.67	1706.70
70 km/h	311.11	1866.67
140 km/h	622.22	1866.67

Map size 4 MB/km		
Speed \ Density	1%	10%
24 km/h	213.33	3413.33
70 km/h	622.22	3733.33
140 km/h	1244.44	3733.33

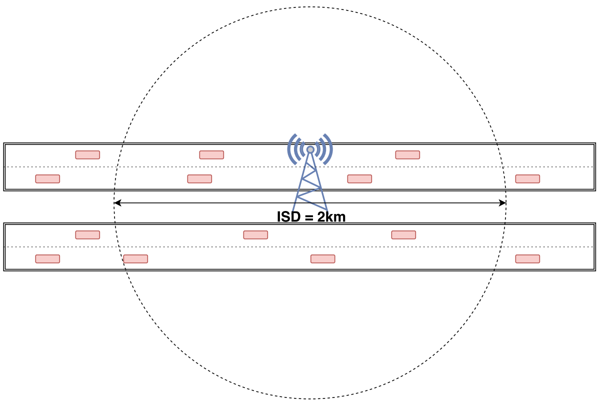

Figure 8: Showing an example scenario of a BS placed close enough to the highway such that it can be assumed the road length is approximately equal to the ISD

Note that the values presented in table 4 are actually per car with HDM capability, and not per car in general. The reliability requirement is set to 95%, which is a stricter version of the quite similar use case ("sensor and state map sharing") presented in the technical report from 3GPP [4].

3.1.3 Remote Driving

To remotely control a car requires a video feed sent from the vehicle. In order to provide a safer transportation, as well as a more natural driving experience for the remote driver, more video streams may be added. Each stream produces a quite hefty throughput in UL, especially when considering minimal latency delay, which makes this use case a very challenging one. On the other side, the data sent from the driver to the car, in the DL, is close to negligible. While the application areas of this use case can be many, the main motivation is to enable an alternative safety system, in case the imagined autonomous vehicle for some reason no longer functions properly.

A few estimations have to be made in order to simulate the use case. First off, it is assumed that each car uses three individual video streams. Two in the front, giving the driver a wide angle of vision, and one that covers the back. Each video stream requires an UL throughput of 3 Mbps, which thereby is summed up to 9 Mbps. Furthermore, it is assumed that the sensor data is kept low and we only consider the video feeds for the UL. A full-blown sensor sharing transmission would drastically increase the data requirement for the UL. The UL throughput requirement of 9 Mbps should be taken with a grain of salt, as it depends on a large set of different assumptions, such as resolution, frames per second, video codec, as well as the total number of video streams. While this throughput requirement represents three video streams in this thesis, for other studies this number might as well correspond to only 1 video stream.

When it comes to the DL, the only necessary data to send is control and sensor feedback. This is done with an interval between 10-100 Hz, but defined as 100 Hz from now on. The data payload is assumed to contain five floats, which yields a bitrate of 2 kB per second. Hence, when considering complete data packets the bitrate is approximated to 20 kbps.

Lastly, an equally important factor to consider is the frequency of occurrence. As the use case strives to act as a back-up system, it is reasonable to assume that it is used with a very low probability. Therefore, in order to capture the worst case scenario in the simulations, the duty cycle is set to 1 %. Since only cars that already have self-driving capabilities installed are able to support this remote control use case, and the prediction for semi-autonomous cars is also 1%, the probability of having a remotely controlled car is only 0.01 %. The requirements for the remote control car use case is summarized in table 5. The strict reliability requirement of 99.999% is based on a technical report from 3GPP [4].

Table 5: Summary of the requirements for the remote control car use case

Downlink	20 kbps
Uplink	9 Mbps
Reliability	99.999 %

3.2 Simulation Scenario

In this section three different topics are considered. First off, it is explained how the automotive map scenario is built and details such as road width generation and car representation are showcased. Secondly, the process of network generation is described, which includes sampling of UEs and deployment of sites. Finally, a table of simulation parameters is presented.

3.2.1 Map Generation

The map used in the simulations is gathered from real world data by using the open source database OSM[1] (OSM). In order to filter out the regions of interest, the API Overpass turbo [2] is used. The roads are divided into different types, where a simple query command in Overpass turbo can sort out the types needed to represent a highway. The query used for generating the road data is as follows,

```
[timeout:25];
(
  way["highway"="motorway"]({{bbox}});
  way["highway"="trunk"]({{bbox}});
  way["highway"="primary"]({{bbox}});
  way["highway"="motorway_link"]({{bbox}});
  way["highway"="primary_link"]({{bbox}});
  way["highway"="trunk_link"]({{bbox}});
);
out body;
>;
out skel qt;
```

where the variable bbox is defined manually using the web-gui. An example is shown in figure 9, where the selected data points are clearly indicated. Furthermore, as is also illustrated in the same figure, data points outside the bounding box are also selected, which is due to the sparse sampling in the OSM database. In short, this means that it is not possible to cut the road exactly as you want, but instead the closest match is selected. Hence, if a specific area of interest is investigated, it is necessary to adjust the data in a post-processing step (cropping).

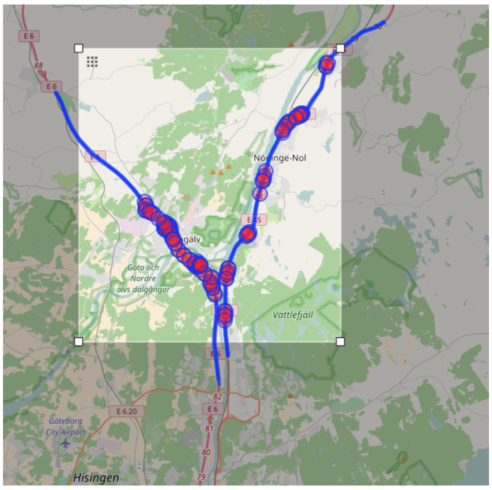

Figure 9: An example of generated data points after running a query on the selected bounding box

The data from OSM is exported as a kml-file, containing a lot of information. Therefore, the first step is to filter out the necessary components from the file and build a new structure. The structure is composed with the following fields:

[1]Map data © OpenStreetMap, see https://www.openstreetmap.org/ and www.openstreetmap.org/copyright
[2]See http://overpass-turbo.eu for more information

Geometry: Used to remove redundant data. Only the data points with the tag 'line' are kept.

Description: Used to decide the road width. The name of the description tag will correspond to one of the filter criteria defined in the query.

Lon and lat: Longitude and latitude coordinates which are used to correctly position the data points and connect them to the real world.

Lanes: Defines the number of lanes of each road segment.

The redundant data is removed according to,

```
myStruct(find(~strcmp({myStruct(1:end).Geometry}, 'Line'))) = []; %Remove redundant data
```

where *myStruct* is the structure containing the fields mentioned above. As previously explained, the exported data from OSM most likely cover a larger area than wanted. In order to cut-out the desired surface, it is first needed to calculate the distance for each side (X,Y) in meters. This can be done using the Haversine formula, which finds the approximate distance between two geographical points (longitude/latitude) in meters.

```
%Distance in X
distX = cord2meter(LatCat(maxLonPos), maxLonValue, LatCat(minLonPos), minLonValue); %meters

%Distance in Y
distY = cord2meter(maxLatValue, LonCat(maxLatPos), minLatValue, LonCat(minLatPos)); %meters
```

The function cord2meter is a matlab implementation based on the JavaScript provided by *Moveble Type* [27] under a common creative licence. The function can be found in Appendix A. It is now possible to cut-out the wanted area size, which for the simulations in question is defined as 5000 meters horizontal and 9000 meters vertical.

The end goal of the map generation, is to build a matrix where each element represents either road or no road. This matrix is of the same size as the surface area, i.e., 5000 columns and 9000 rows. If a 1-by-1 meter representation is desired, the sparse data points from OSM need to be interpolated. This is done with the following lines,

```
neededPoints = arclength(centralLineLon,centralLineLat); %The number of points we actually need

actualPoints = length(centralLineLon); %The number of points we currently have from the sampled data

%Here we do the interpolation, designed to fit into the map
centralLineLonMap = interp(centralLineLon,round(neededPoints/actualPoints));

centralLineLatMap = interp(centralLineLat,round(neededPoints/actualPoints));
```

where centralLineLon and centralLineLat correspond to a road segment found in one of the cells in the myStruct fields *longitude* and *latitude*. The function *arclength* calculates an approximation of needed data points for placing the road segments in the map matrix. This is done using a cumulative chordal distance algorithm illustrated in figure 10.

In order for the matlab interpolation function *interp* to work, the road segments need to be of a length greater than nine. Hence, for shorter segments, different methods are used in order to expand the number of elements. Appendix B shows one of the methods, where a segment is of a length lesser than nine. Note that the same code needs to be run for both the longitude and latitude segment data.

By reading the *description* tag for each segment the road width is defined. For highway types,

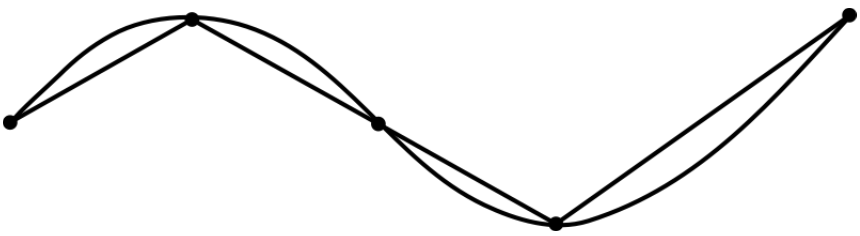

Figure 10: Basic illustration for calculating the arc-distance by summing up linear segments

the width is approximated to four meters per lane. This is based on the minimum lane width set by the federal highway roads in Germany (bundesstraße), which is defined as 3.5 meters plus 0.5 meters for the side region [28].

In order to insert the side points of the road to the map matrix, and fill the area in-between these points, they first need to be correctly defined. As illustrated in figure 11, the points should be shifted 90 degrees in relation to the current road curvature. Hence, these data points are calculated according to,

```
function [pos1, pos2] = getRoadWidthPos(point1,point2,roadWidth)

angle = atan2(point2(2)- point1(2), point2(1) - point1(1)) * 180 /pi;

theta = deg2rad(angle-90);

x_out1 = point1(1) + roadWidth/2*cos(theta);
y_out1 = point1(2) + roadWidth/2*sin(theta);

x_out2 = point1(1) - roadWidth/2*cos(theta);
y_out2 = point1(2) - roadWidth/2*sin(theta);

pos1 = [x_out1, y_out1];
pos2 = [x_out2, y_out2];

end
```

where the distance to a point is the road width divided by half. By building a polygon between these two points and the previous two points, it is possible by using matlab's built-in function *inpolygon* to find the matrix elements inside the polygon and fill them accordingly (figure 12b).

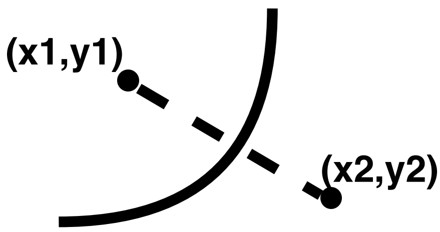

Figure 11: When the road is turning the position of the road side points need to shift accordingly. The bent curve represents the center of the road

The matrix, consisting of zeros and ones will look similar to the one shown in figure 12a. The ones are displayed as white color and the zeros as black. For the next step, each matrix element undergoes a simple algorithm which generates a 2-by-2 square per element. The top left position of each square is set to a number which represents either *in* or *out*, this selection depends on the previous element values covered by the same square size. In this fashion, it is possible to separate the bins from being inside or outside the motorway, while at the same time enabling four use cases to be simulated separately. If more than four use cases are to be simulated, a 3-by-3 square would be needed (enabling a total of nine cases). By comparing figure 12b and figure 13, it is clearly shown that the road is no longer filled, providing space for additional inputs. The code for the square creation algorithm can be found in appendix C.

(a) (b)

Figure 12: (a) Showcasing an example of how a road map matrix may look like. If observed closely, it can be noticed that the white lines correspond to four lanes. (b) Zoomed in section of the left side roads in image (a), as seen the roads are completely filled

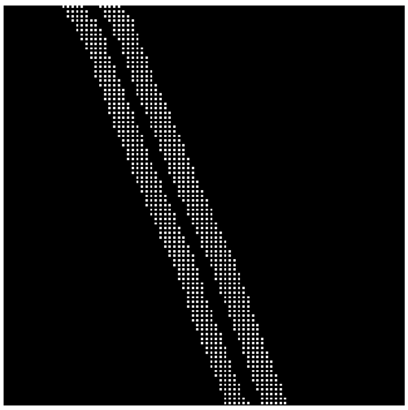

Figure 13: The road segments after modification. The roads are no longer completely filled. For illustration purposes the non-motorway area is set to zero (black), which is not the case in reality

To add more detail to this process, figure 14a illustrates how one square of the large matrix looks like after the previously mentioned algorithm. By taking the probability data, found in section 3.1, for each of the two remaining use cases, the matlab function *datasample* is used to randomly distribute sample points without replacement. Each square can be seen as a potential car, where the blocks indicate which communication is active for this specific unit. For example, one square may contain only MBB traffic, while another, as seen in figure 14b, may contain traffic from MBB, HDM and RD. Since only three use cases are investigated in this thesis, the fourth block will always remain as zero.

(a) (b)

Figure 14: (a) A set of four squares, which represent a potential car. In this case only data from the MBB use case is transmitted, this is also how all squares look before adding the randomly placed bins from use case 2 and 3. (b) An example where all three use cases are active. Note that all blocks are mutually selected as either *in* or *out*, which is a criterion when assigning the random bins

3.2.2 Network Generation

This section is about building the network, where two subjects are highlighted; sampling the UEs and deploying the BS sites. The first of the two touches the balance between getting as accurate results as possible, while not letting the computation time grow too large. As the generated map is of great size (45 million bins), it is not suitable to sample all the data points. As a matter of fact, most of the bins can be discarded. It is however important to not discard valuable (rare) data points, such as the ones carrying data from the RD use case. Different sampling factors are used depending on the use case and whether or not the data points are located inside or outside the motorway. For instance, 100% of the HDM and RD data points inside the motorway are sampled, while only 1% and 10% respectively are sampled outside the motorway. This boils down by the fact that the motorway covers only a fraction of the total map area, making these samples quite rare, and thus important. Hence, in order to generate simulation results that are statistically sufficient 100% of the samples are saved.

The deployment of the BS sites are based on statistics from real world data. By inspecting various regions alongside the motorway in different European countries, it was noticed that the ISD variation was very large, but typically between 2 and 4 km. For the simulations in this thesis the focus is on an ISD of 2 km. While this distance can be found in the real world, it is important to keep in mind that a much larger distance between sites is frequently seen. The placement of the sites have been manually positioned in a logical fashion. Figure 15 shows the deployment of the sites together with the sampled UEs for each use case. As made clear the RD samples inside the motorway are very sparse, in this specific plot only 93 samples are computed, where an HDM probability of 10 % is assumed.

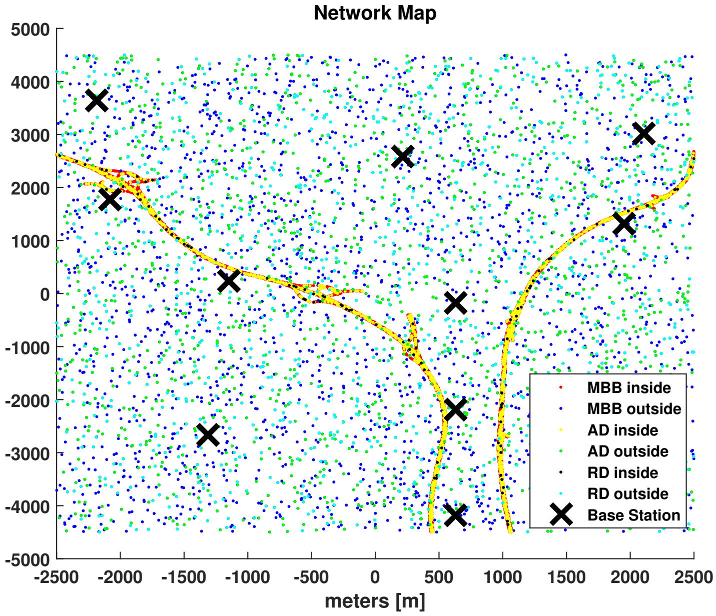

Figure 15: Network map showing the sites, the UEs and the map itself

The direction of each individual antenna is manually adjusted to collectively cover as large part of the highway as possible. By using the following method it is possible to get an indication of a good antenna direction setup:

1. Sum the number of users served by each cell separately
2. Re-direct the antennas in a logical fashion
3. Go back to step 1 and look if the three cells used by each site are better equalized than before. Repeat until no clear change is made visible.

The above method could possibly be made into a script by calculating the variance, but the manual approach is used for this thesis. An example of a histogram over the number of users per cell can be seen in figure 16. Every third bar represents a new site. As can be noted, some of the cells have a low utilization, which is due to the fact that they are not directed towards the highway.

When it comes to the tilt T of the antennas, it is calculated by deriving the angle when pointing the beam towards the cell-edge,

$$T = \text{round}(\arctan(\frac{h}{\frac{1}{2} \cdot ISD}) \cdot \frac{180}{\pi}), \tag{14}$$

where h is the BS height, which is set to 30 meters. With the ISD defined as 2 km, the tilt is calculated to 2°

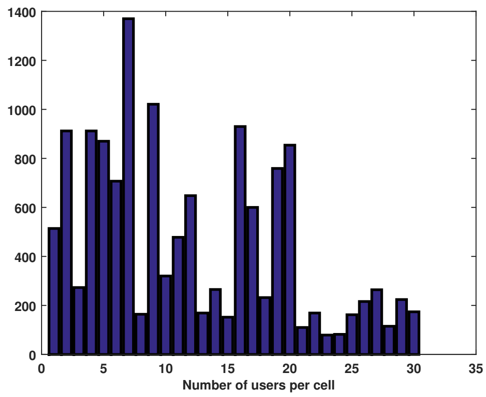

Figure 16: The total number of served users per cell. Each bar represent a cell, and every three consecutive bars correspond to a site

3.2.3 Simulation Parameters

A significant amount of system variables are manipulated and experimented with. Table 6 summaries the general simulation parameters.

Table 6: Various simulation parameters for the NR and LTE cases. Values being centered indicate that they are valid for both the LTE and NR simulations

	LTE: 800 MHz, 1800 MHz	**NR: 3.5 GHz**
Map (terrain)	Flat	
Macro cell layout	ISD 2km: 10 sites (30 cells), ISD 4km: 4 sites (12 cells)	
ISD (inter-site distance)	2 km, 4 km	
Outdoor to in-car penetration loss	9dB	
User distribution	Randomly and uniformly distributed over area	
Car density	Outside: 100 cars/km2. Inside: velocity dependant	
Macro BS output power	40 W per 20 MHz BW	100 W
Macro BS antenna configuration		SA = 8x1 AOSA = 2x8
Macro BS antenna height	30 m	
Macro BS electrical downtilt	Pointing at cell edge	
Macro BS mechanical downtilt	0°	
Macro BS BF type	N/A	DL: Grid-of-beams, UL: MRC
Bandwidth	20 MHz	100 MHz
Duplex	FDD	TDD DL 20%, 30%, 50%
DL number of streams	Up to 2	
DL highest modulation	256 QAM	
UL number of streams	1	
UL highest modulation	64 QAM	
Propagation type	ITU RMa	
UE number of Tx	1	
UE number of Rx	2	
UE output power	23dBm	
UE antenna model	isotropic	
UE antenna gain	-8dBi	-3dBi
UE antenna height	1.5m above ground	

4 Simulation Results

The ambition of this section is to showcase simulation results from the automotive scenario when using different technology setups. In order to ease the reading throughout the section, each setup is assigned an index, which can be found in table 7. Furthermore, as many simulation combinations are investigated, tables of results have been constructed in order to facilitate the key takeaways. These summary of results for MBB, HDM and RD can be found in appendices E, F and G respectively. The section starts off by investigating which array configuration is most applicable for this automotive scenario. Afterwards a complete performance evaluation for each use case is made when sharing the same spectrum as MBB users. Then the possibility of deploying a dedicated V2N carrier is investigated and lastly the section ends with a brief analysis of UE output power.

Table 7: Showing all the used setups. Each setup is assigned a letter, for future reference

Setup index	Setup configuration
A	LTE 800 MHz 20 MHz BW
B	LTE 1800 MHz 20 MHz BW
C	NR 3.5 GHz 100 MHz BW TDD DL ratio 50%
D	LTE 800 MHz + LTE 1800 MHz 40 MHz BW
E	LTE 800 MHz + NR 3.5 GHz 120 MHz BW TDD DL ratio 50%
F	LTE 800 MHz + NR 3.5 GHz 120 MHz BW TDD DL ratio 30%
G	LTE 800 MHz + NR 3.5 GHz 120 MHz BW TDD DL ratio 20%

4.1 Simulation of Array Configuration

As discussed in section 2.1.3, the array configuration acts as an vital integral for the simulation results. Different setups suit different scenarios. In figure 17 MBB performance is evaluated by plotting the user throughput in Mbps as a function of traffic per square meter, for both DL and UL. During these simulations all use cases are active and the vehicle velocity is fixed to 70 km/h. As made evident, the SA = 8x1, AOSA = 2x8 structure performs the best in this automotive scenario. This is most likely because the majority of the UEs are contained along a straight path, which makes the horizontally tall configuration ideal. However, this configuration is of high complexity, as it requires $8 \cdot 1 \cdot 2 \cdot 8 = 128$ antenna elements. Hence, when keeping complexity (and cost) in mind, the SA = 2x1, AOSA = 8x4 setup may be favourable. The following simulations are aiming to capture the best performing scenarios, which is why all the next NR simulations use the SA = 8x1, AOSA = 2x8 configuration.

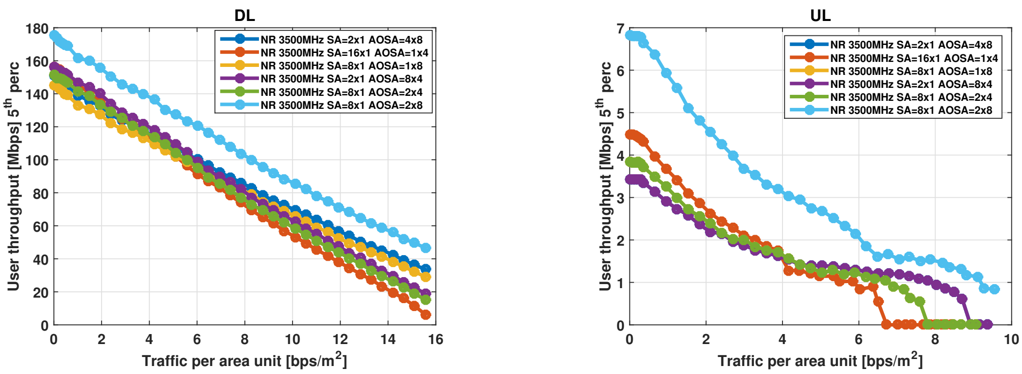

(a) (b)

Figure 17: Transmission using setup C with different array configurations (a) DL (b) UL

4.2 Co-channel Deployment

With co-channel deployment it means that the V2N use cases are using the same carrier(s) as the MBB users. Three different topics are considered in this section. First off, the impact on MBB performance when increasing the network load per use case is showcased. Secondly, an evaluation of HDM performance is made, and lastly a performance analysis of the RD use case. For the HDM case, the velocity is iterated, while for the cases of MBB impact and RD the velocity is fixed to the worst-case scenario (v = 24km/h). The opposite of using a co-channel deployment is to use a dedicated carrier, which is investigated in section 4.3.

4.2.1 Impact on MBB

A vital aspect to consider, is how the current MBB traffic is affected by adding new use cases. In this section it is investigated how the MBB performance is impacted, and if the 2022 MBB requirement can be fulfilled when co-existing with the V2N use cases. While simulation parameters such as HDM packet size, HDM/RD vehicle density and CA are varied, the vehicle velocity is kept constant at v = 24 km/h. By using the lowest vehicle velocity, we are able to capture a worst-case scenario. Since the following simulations are focusing on MBB performance, a 95% reliability is assumed (i.e 5-percentile).

The starting point of this evaluation is to simulate the impact when using a standalone LTE carrier, setup A, and a parameter configuration representing the lowest communication scenario. This is shown in figure 18, where the HDM density is set to 1% and the packet size to 10 kB/km. As can be seen the 2022 MBB requirement can not be completely fulfilled in the DL. Furthermore, the MBB performance in UL is not impacted much when HDM and RD communications are added.

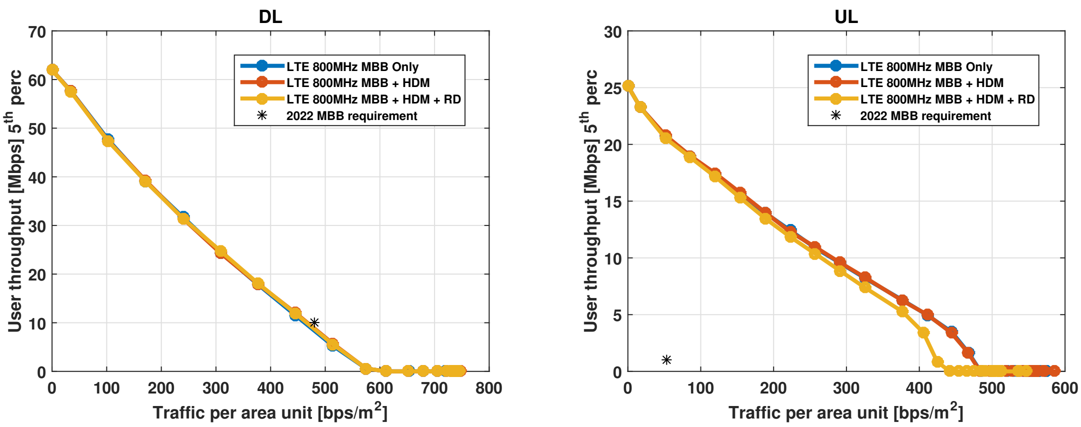

(a) (b)

Figure 18: User throughput as a function of traffic per area unit when using setup A. The HDM vehicle density is set to 1% and the map data size 10 kB/km (a) DL (b) UL

Even though the DL requirement is not fulfilled, it may be of interest to still investigate the impact trend when increasing the HDM density to 10%. Hence, figure 19 showcases this scenario. As clearly shown, the MBB performance in the UL is now greatly impacted from the large amount of communicating vehicles.

It is now of interest to investigate if using CA would boost the MBB performance, allowing both the DL and UL to fulfill the 2022 requirement. For the next simulations setup D is used. Figure 20 shows the scenario where 1% of the cars are transmitting HDM packets, while figure 21 shows

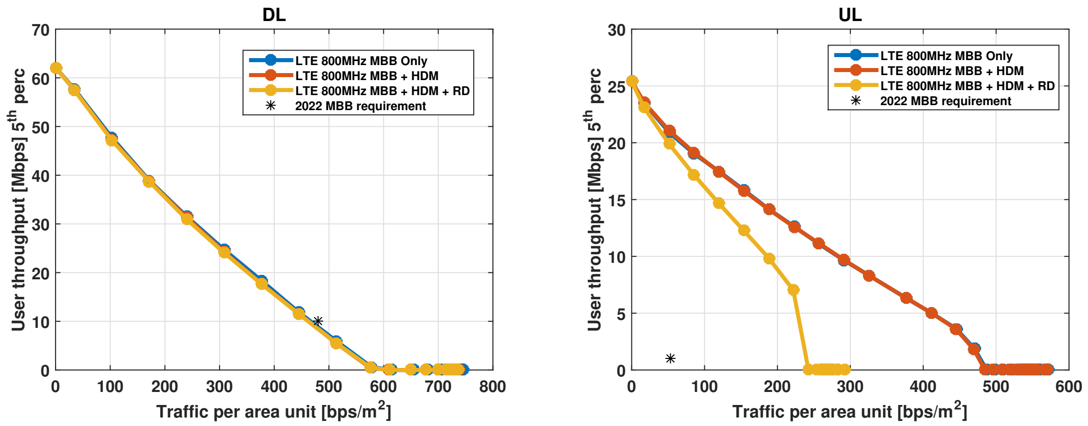

(a) (b)

Figure 19: User throughput as a function of traffic per area unit when using setup A. The HDM vehicle density is set to 10% and the map data size 10 kB/km (a) DL (b) UL

the same setup, but 10% of HDM vehicles instead. As is illustrated in these figures, by using CA the MBB 2022 requirement is easily met both in the DL and UL.

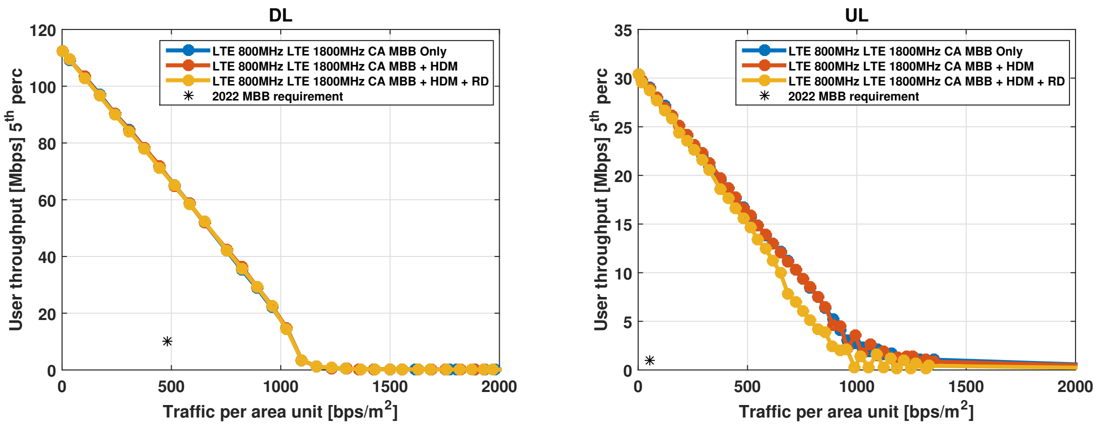

(a) (b)

Figure 20: User throughput as a function of traffic per area unit when using setup D. The HDM vehicle density is set to 1% and the map data size 10 kB/km (a) DL (b) UL

The next step is to let the HDM packet size grow to 4 MB/km instead of 10 kB/km, which will yield a much greater interference for the MBB traffic. While the LTE CA setup can still support the scenario of having 1% HDM cars, the impact on MBB performance is still quite low, but now more visible. This can be seen by comparing figure 20 and figure 22. Since 1% HDM vehicles is a relative low number of cars, the impact of going from 10 kB to 4 MB per km is not clearly showcased in the previously mentioned figures. Hence, by letting the HDM car density increase to 10%, the packet size change is distinctly shown. As seen in figure 23, the impact is enormous, and the 2022 MBB DL requirement can no longer be fulfilled.

An interesting step of the MBB impact evaluation is to investigate how the implementation of NR technology would benefit in comparison to the previously mentioned setup. The next simulation uses cross-technology CA, as seen in setup E, and the array configuration chosen in section 4.1. By inspecting figure 24, it is made clear that this system setup is able to fulfill the 2022 MBB requirement in both DL and UL, despite the large impact from the V2N use cases (here using 10%

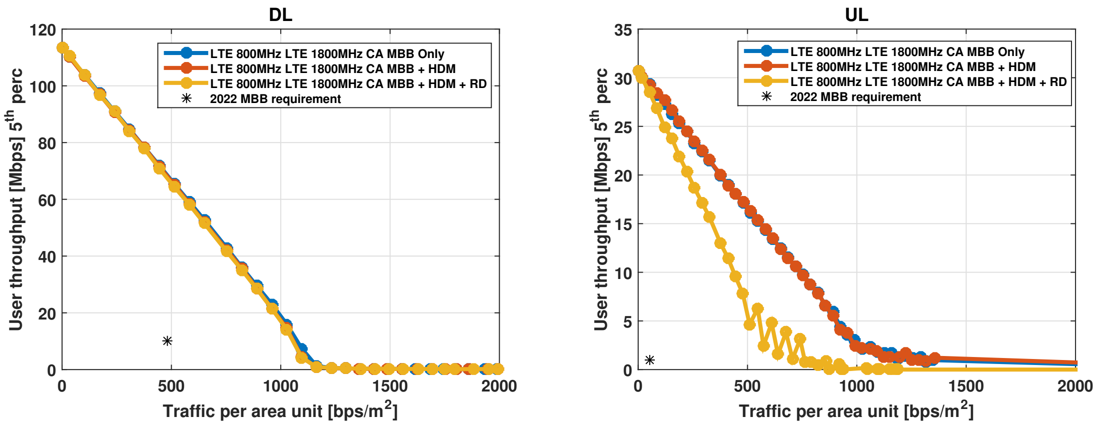

(a) (b)

Figure 21: User throughput as a function of traffic per area unit when using setup D. The HDM vehicle density is set to 10% and the map data size 10 kB/km (a) DL (b) UL

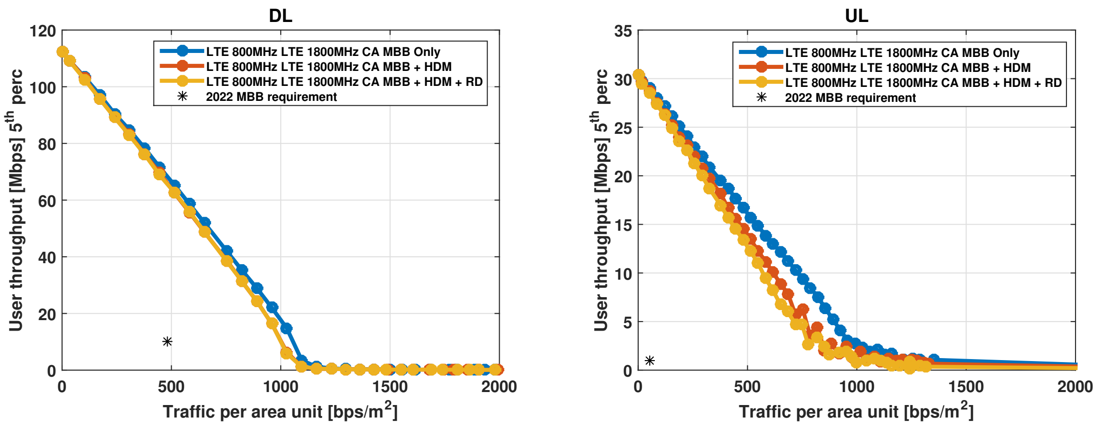

(a) (b)

Figure 22: User throughput as a function of traffic per area unit when using setup D. The HDM vehicle density is set to 1% and the map data size 4 MB/km (a) DL (b) UL

HDM cars and 4 MB/km).

Furthermore, coverage maps over both DL and UL transmission are illustrated in figure 25 and 26. As can be seen, the LTE+NR setup is performing better both in DL and UL when it comes to average and cell-edge (5%-tile) peak throughput. However, the difference in UL is very small.

Lastly, a CDF curve over the DL beamforming path gain for setup C can be seen in figure 27. The beamforming path gain corresponds to the total gain, as previously discussed in section 2.1.3, i.e element gain + SA gain + array gain.

4.2.2 Impact on MBB with large ISD

As explained before in section 3.2.2, the typical ISD along the inspected highways varied between 2 and 4 km. This section acts as motivation for why a larger ISD of 4 km is not considered in the main part of the simulations.

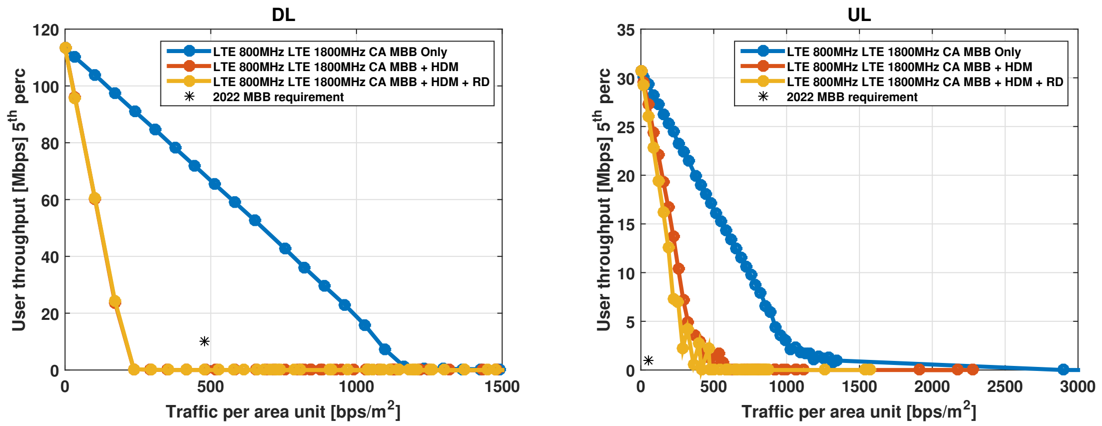

(a) (b)

Figure 23: User throughput as a function of traffic per area unit when using setup D. The HDM vehicle density is set to 10% and the map data size 4 MB/km (a) DL (b) UL

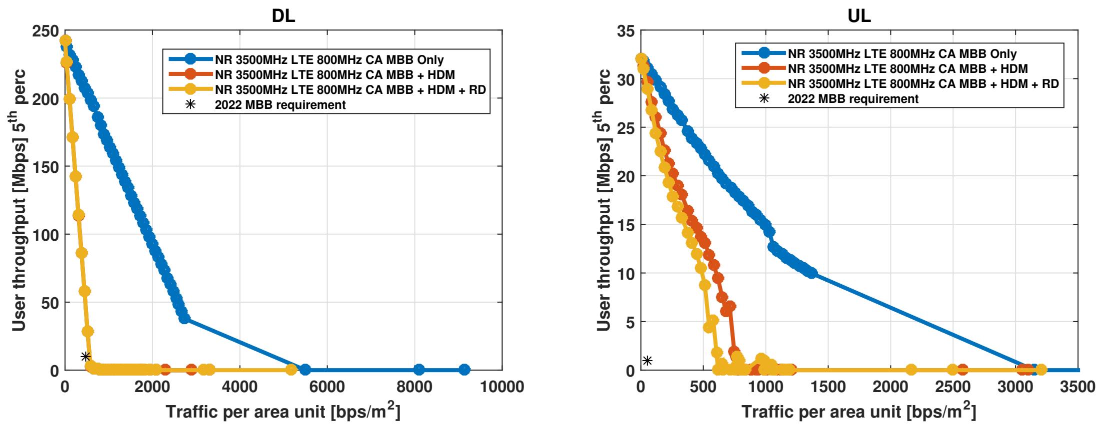

(a) (b)

Figure 24: User throughput as a function of traffic per area unit when using setup E. The HDM vehicle density is set to 10% and the map data size 4 MB/km (a) DL (b) UL

By running a simulation using the best-performing setup (based on the simulations when using ISD = 2 km), setup E, it is discovered that the 2022 MBB requirement is not fulfilled, which is pictured in figure 28. Hence, running simulations for other system setups is deemed as redundant.

Coverage plots for both DL and UL transmission have also been computed, and can be found in appendix D.

4.2.3 Performance of HDM

In this section the performance of the HDM use case is put under the glass. For this performance evaluation the velocity, as well as the size of the map data are varying. It is observed in figure 29 and 30 that when using setup D for a low velocity, only the case with low HDM probability is able to meet all three data size requirements. When it comes to the case of 10% HDM probability, neither the 2 MB/km nor the 4 MB/km requirements can be met in the DL, as seen in figure 30a.

The same setup (probability of 10%) is now used for a velocity of v = 70 km/h. By inspecting

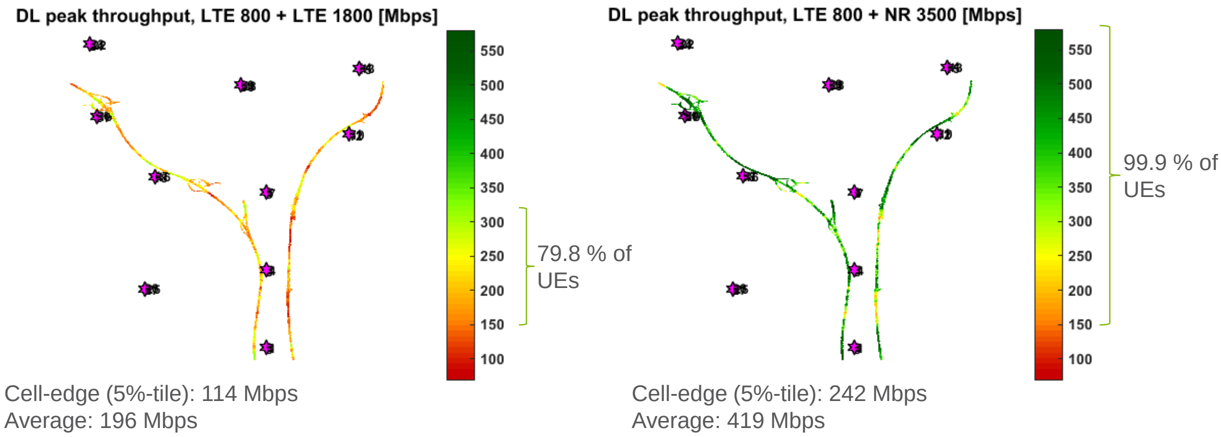

Figure 25: Coverage map: DL peak throughput for setup D and E. Average and cell-edge throughput is shown for each setup, as well as the percentage of UEs which experience 150 Mbps or more. The ISD is set to 2 km

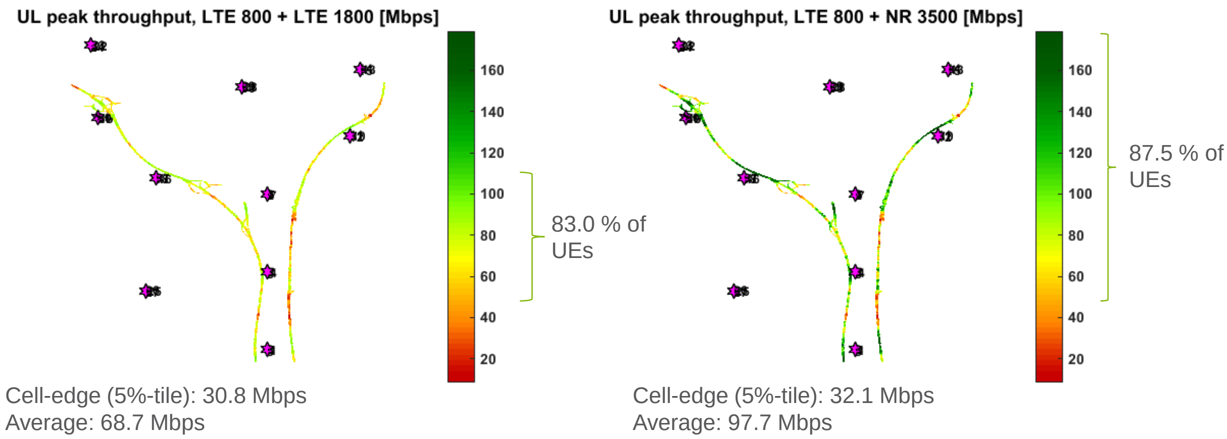

Figure 26: Coverage map: UL peak throughput for setup D and E. Average and cell-edge throughput is shown for each setup, as well as the percentage of UEs which experience 50 Mbps or more. The ISD is set to 2 km

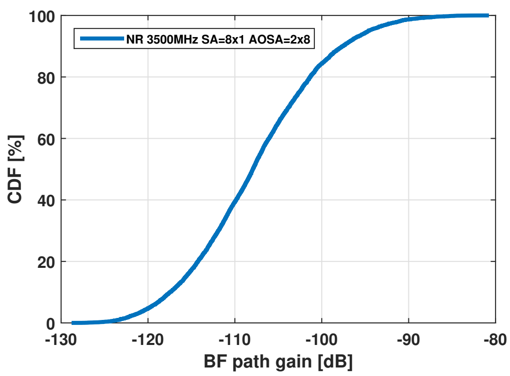

Figure 27: CDF for the DL beamforming path gain when using setup C

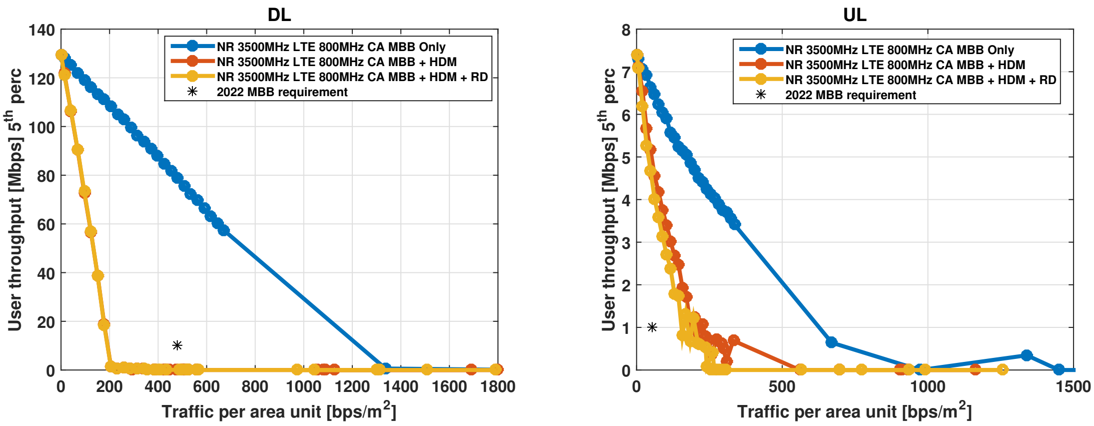

(a) (b)

Figure 28: User throughput as a function of traffic per area unit when using setup E. The HDM vehicle density is set to 10%, the map data size is set to 4 MB/km and the ISD is 4 km (a) DL (b) UL

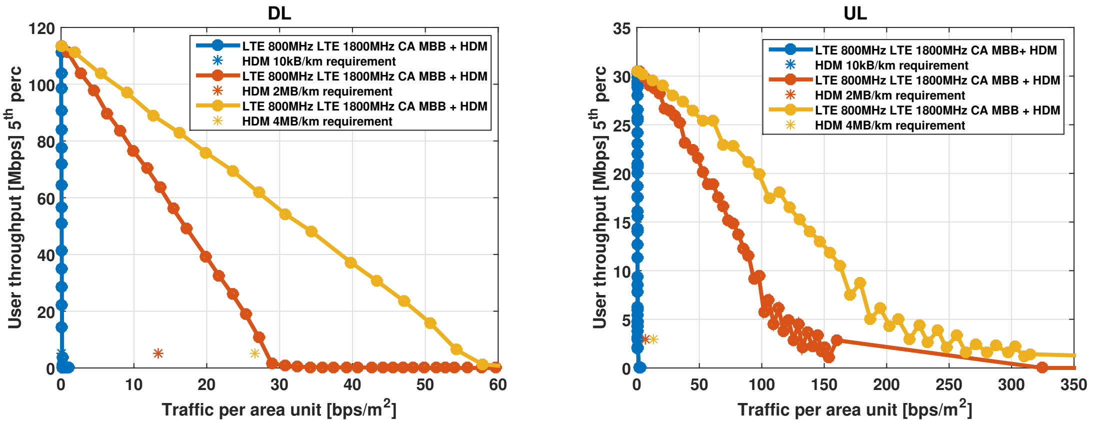

(a) (b)

Figure 29: User throughput as a function of traffic per area unit when using setup D. The HDM vehicle density is set to 1% and the velocity is 24 km/h (a) DL (b) UL

figure 31 it is noticed that the requirement for 2 MB/km data transmission is now fulfilled. The velocity, and thus the vehicle density is clearly affecting the performance. Moreover it is noticed that the 4MB/km case is still not fulfilled.

In similar fashion a performance boost is achieved when using a velocity of 140 km/h, but as seen in figure 32, even when having this high velocity (and thus fewer cars), the 4 MB/km requirement cannot be fulfilled.

By again setting the velocity to 24 km/h and using an HDM probability of 10%, but this time switching to a NR standalone system, setup C, it is made visible in figure 33a that even with this technology the 4 MB/km requirement is not satisfied. Furthermore, figure 33b indicates that using this setup the 2022 MBB requirement is also not fulfilled.

As pictured in figure 34, when using the NR standalone setup and iterating over all velocities while setting the map data size to 4 MB/km, it is noticed that only the $v = 24$km/h requirement is unsatisfactory.

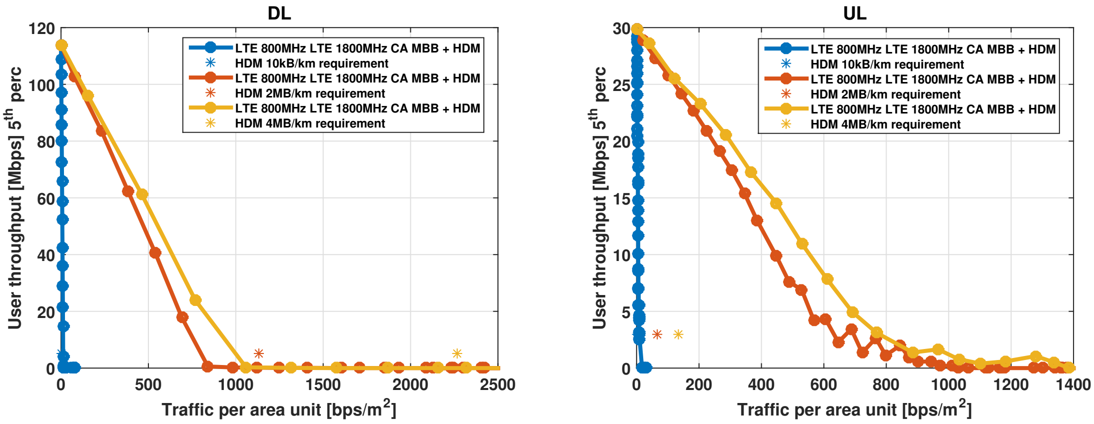

(a) (b)

Figure 30: User throughput as a function of traffic per area unit when using setup D. The HDM vehicle density is set to 10% and the velocity is 24 km/h (a) DL (b) UL

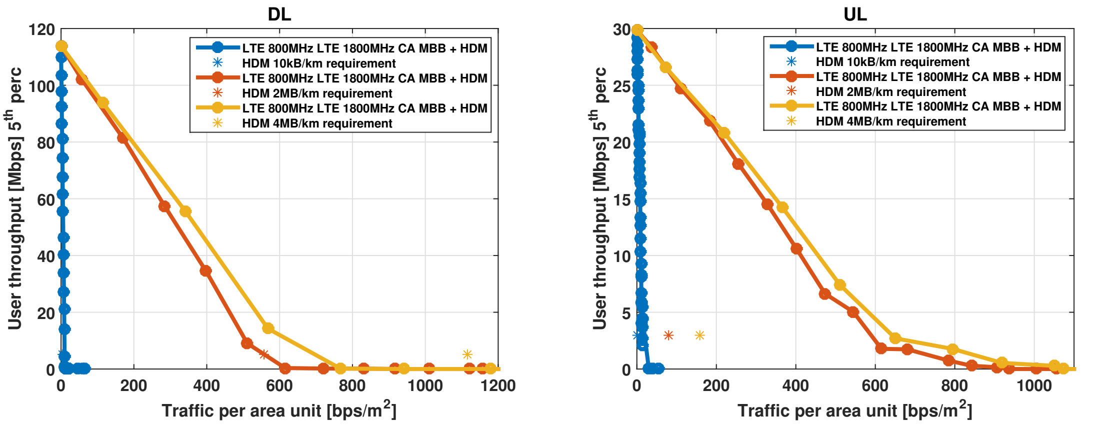

(a) (b)

Figure 31: User throughput as a function of traffic per area unit when using setup D. The HDM vehicle density is set to 10% and the velocity is 70 km/h (a) DL (b) UL

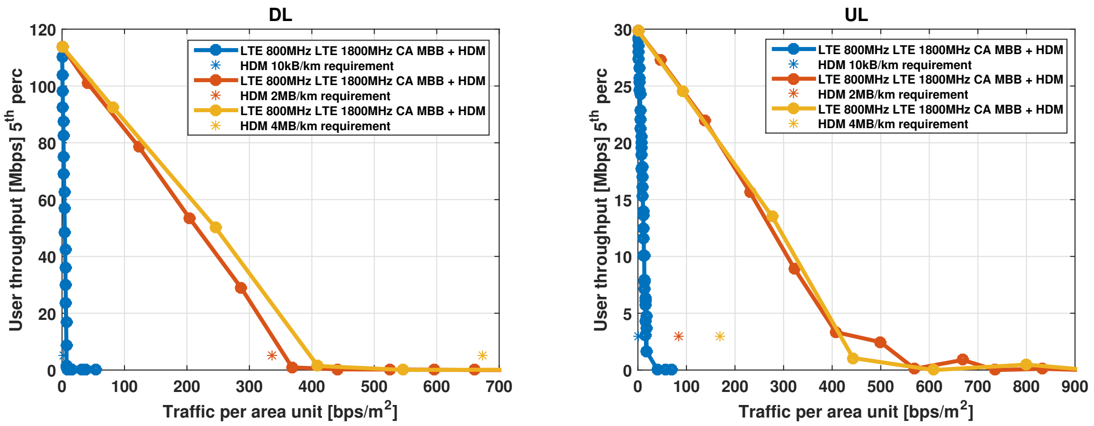

(a) (b)

Figure 32: User throughput as a function of traffic per area unit when using setup D. The HDM vehicle density is set to 10% and the velocity is 140 km/h (a) DL (b) UL

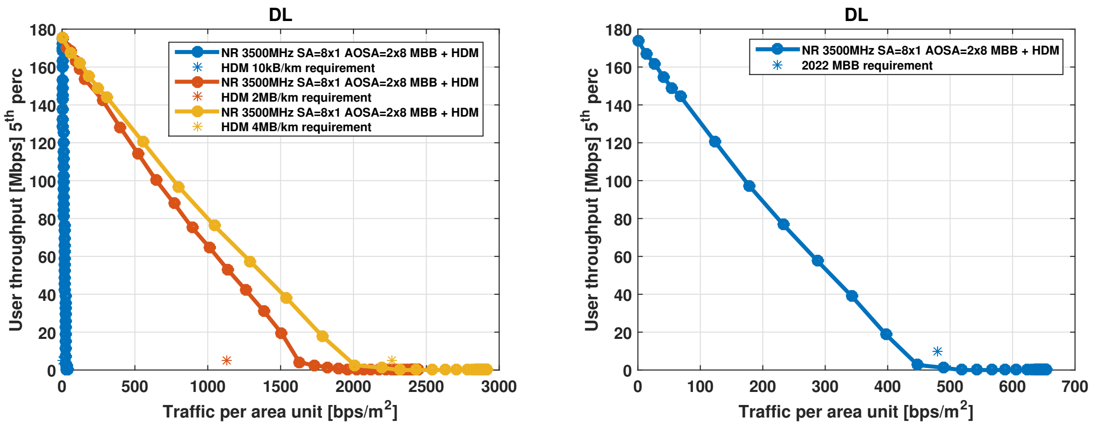

(a) (b)

Figure 33: User throughput as a function of traffic per area unit when using setup C. The HDM vehicle density is set to 10% and the velocity is 24 km/h (a) Performance of HDM (b) Performance of MBB

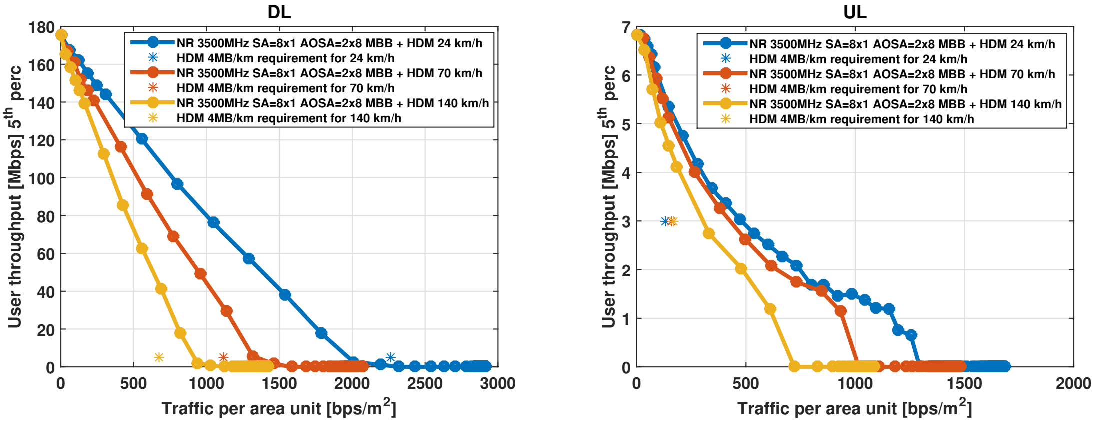

(a) (b)

Figure 34: User throughput as a function of traffic per area unit when using setup C. The HDM vehicle density is set to 10% and the map data size is set to 4 MB/km (a) DL (b) UL

Lastly, a performance evaluation is made when using setup E. As made clear in figure 35, this system setup manages to satisify all HDM requirements, even the 4 MB/km case (v is set to 24 km/h to capture the toughest scenario). Furthermore, as is illustrated in figure 36, this setup also fulfills the 2022 MBB requirement.

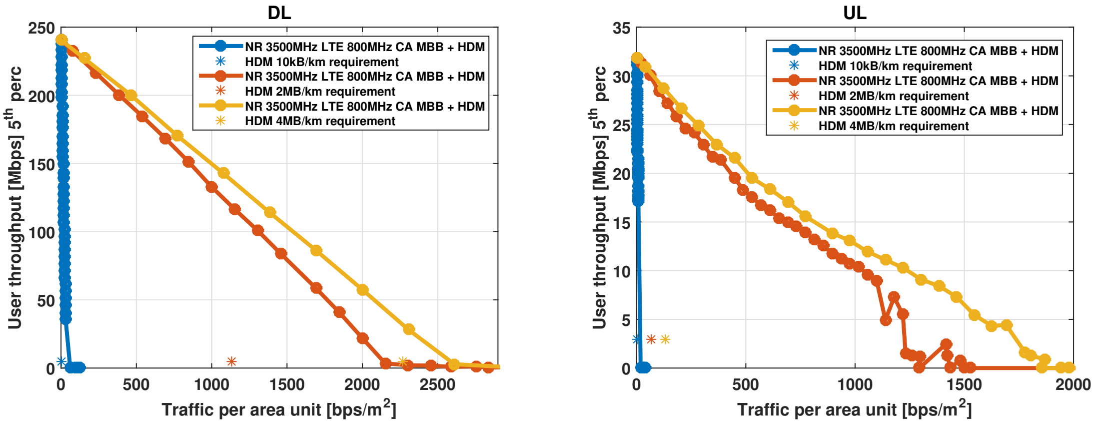

(a) (b)

Figure 35: User throughput as a function of traffic per area unit when using setup E. The HDM vehicle density is set to 10% and the vehicle velocity is set to 24 km/h (a) DL (b) UL

4.2.4 Performance of RD

In this section the performance evaluation of the RD use case is shown. For each presented simulation throughout this section, the velocity has been set to 24 km/h. Just like the performance analysis of HDM, both the density of HDM/RD cars and data sizes for HDM transmission are iterated. The reason for the latter is due to the fact that having a larger data size for the high definition maps is impacting the RD performance due to interference. However, only the two cases of 10 kB/km and 4 MB/km are investigated (for 4 MB/km simulations see section 4.3.2 and appendix G). In similar fashion as the HDM evaluation, the first setup that is considered is setup D. Figure 37 showcases this scenario, where a map data size of 10 kB/km and a HDM car

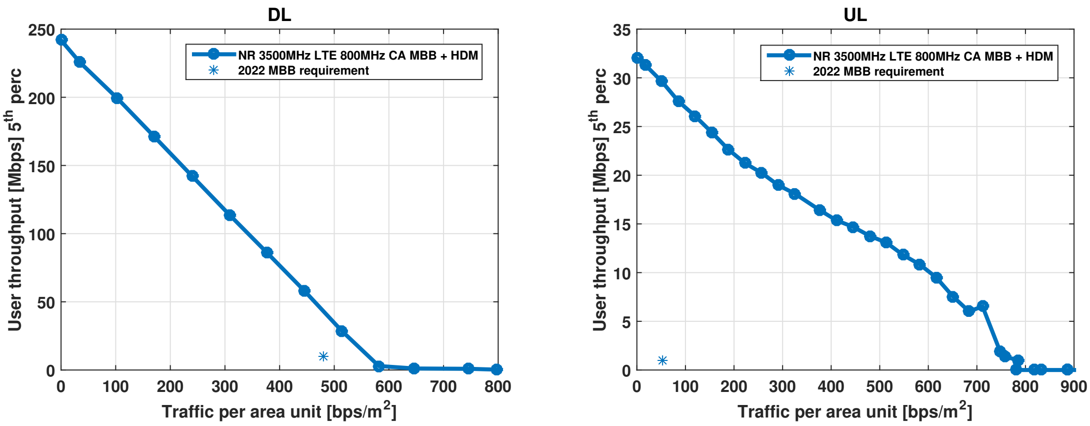

(a) (b)

Figure 36: User throughput as a function of traffic per area unit when using setup E. The HDM vehicle density is set to 10% and the vehicle velocity is set to 24 km/h (a) DL MBB impact (b) UL MBB impact

probability of 1% are being used. As can be seen, the RD requirement is fulfilled for this setup. However, when increasing the number of RD cars by letting the HDM car probability grow to 10%, the requirement can no longer be satisfied in the UL, as pictured in figure 38. Notice that the 0.001-percentile is being used for each RD simulation (due to the reliability requirement of 99.999%).

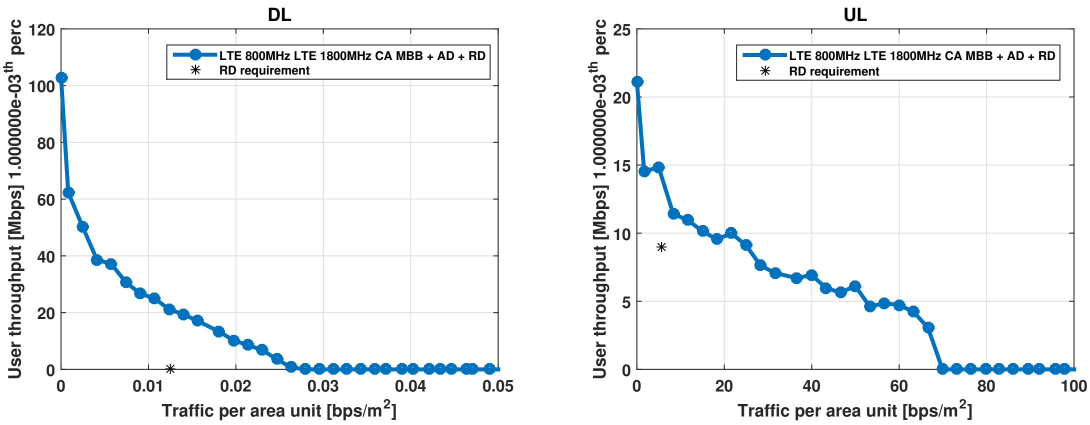

(a) (b)

Figure 37: User throughput as a function of traffic per area unit when using setup D. The HDM vehicle density is set to 1% and the map data size is set to 10 kB/km (a) DL (b) UL

As setup D did not meet the UL requirement, instead setup E is being simulated in figure 39 and 40, where an HDM car probability of 1% and 10% are respectively used. As seen in these figures, the LTE+NR interworking setup is performing better, but is also struggling in the UL, which cannot fulfill the RD requirement. Furthermore, figure 41 is showing the impact of going from LTE 800MHz standalone, to NR 3500MHz standalone, and to LTE 800MHz + NR 3500 interworking. In order to fulfill the UL requirement, a solution to this scenario is to lower the NR TDD DL ratio, and thus giving more resources to the UL. This is showcased in figure 42 by using a setup G. As is illustrated, the RD requirement is fulfilled when lowering the TDD DL ratio to 20%. However, an important aspect to consider is that MBB traffic is DL heavy, and a lower TDD

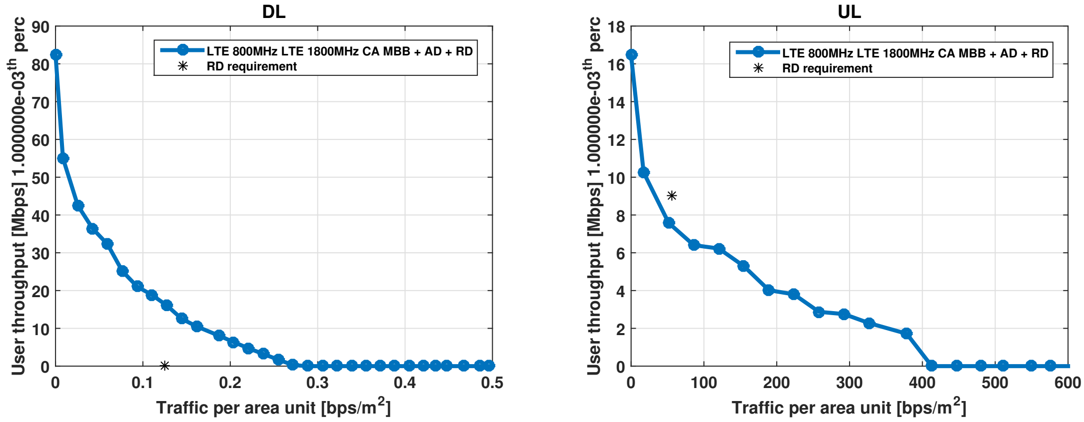

(a) (b)

Figure 38: User throughput as a function of traffic per area unit when using setup D. The HDM vehicle density is set to 10% and the map data size is set to 10 kB/km (a) DL (b) UL

DL ratio is thus not favourable. The impact on MBB when using this ratio is shown in figure 43, which tells that the 2022 requirement is indeed satisfied. However, when increasing the map data size to 4 MB/km, as done in figure 44, this configuration is no longer possible as the MBB requirement is far from being fulfilled. A possible solution to this concern is to rely on a dedicated carrier, which is investigated in the following section.

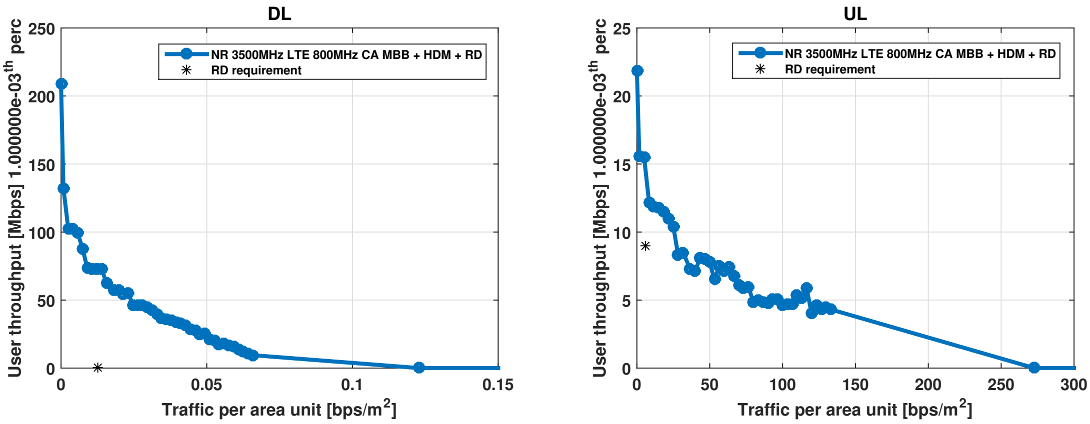

(a) (b)

Figure 39: User throughput as a function of traffic per area unit when using setup E. The HDM vehicle density is set to 1% and the map data size is set to 10 kB/km (a) DL (b) UL

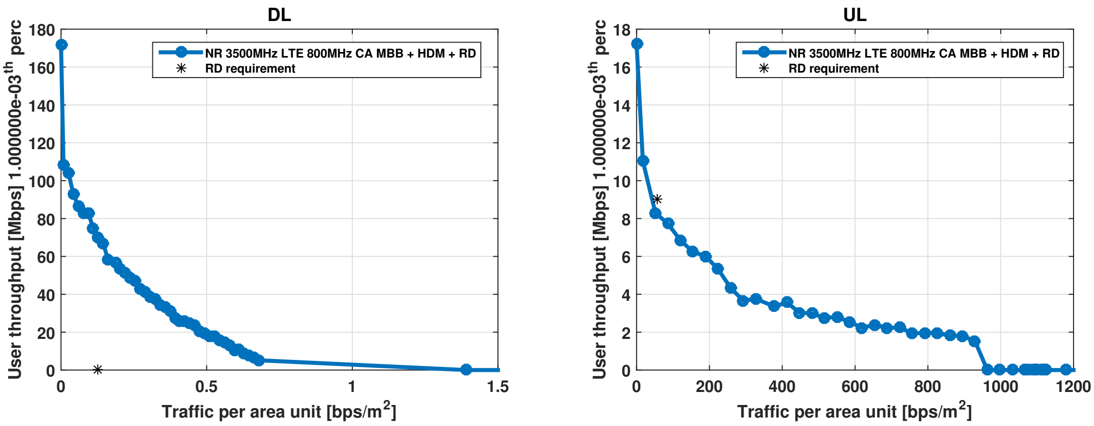

(a) (b)

Figure 40: User throughput as a function of traffic per area unit when using setup E. The HDM vehicle density is set to 10% and the map data size is set to 10 kB/km (a) DL (b) UL

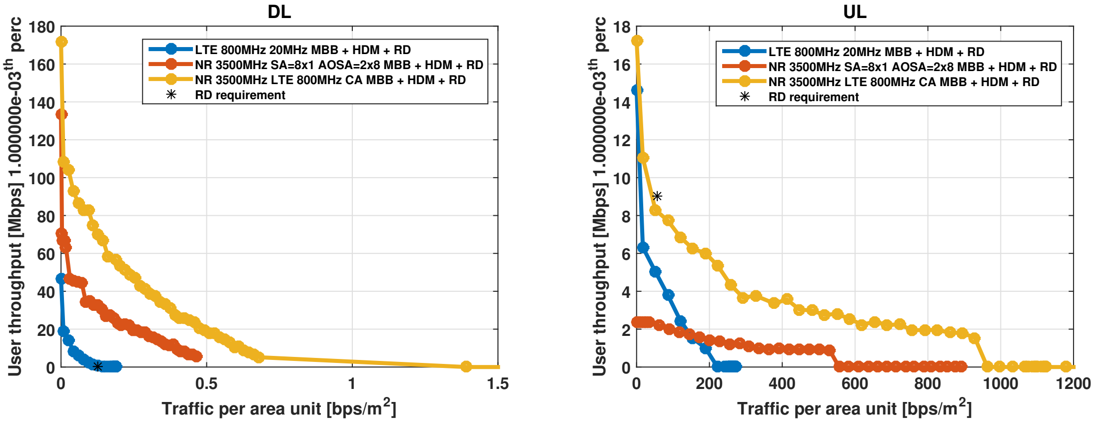

(a) (b)

Figure 41: Showcasing the affect of adding additional technologies, going from LTE standalone to NR standalone and lastly LTE-NR interworking (setup A, C and E). The HDM vehicle density is 10% (a) DL (b) UL

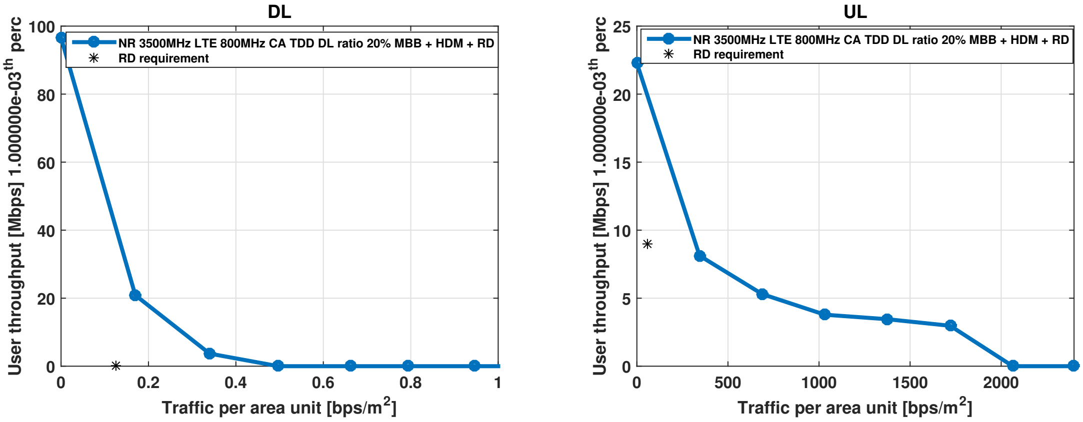

(a) (b)

Figure 42: User throughput as a function of traffic per area unit when using setup G. The HDM vehicle density is set to 10% and the map data size is set to 10 kB/km (a) DL (b) UL

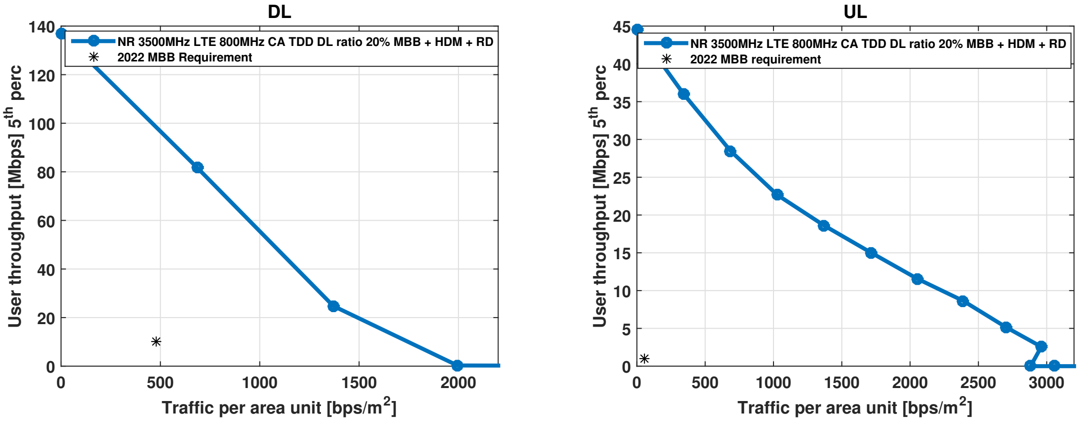

(a) (b)

Figure 43: User throughput as a function of traffic per area unit when using setup G. The HDM vehicle density is set to 10% and the map data size is set to 10 kB/km (a) DL MBB impact (b) UL MBB impact

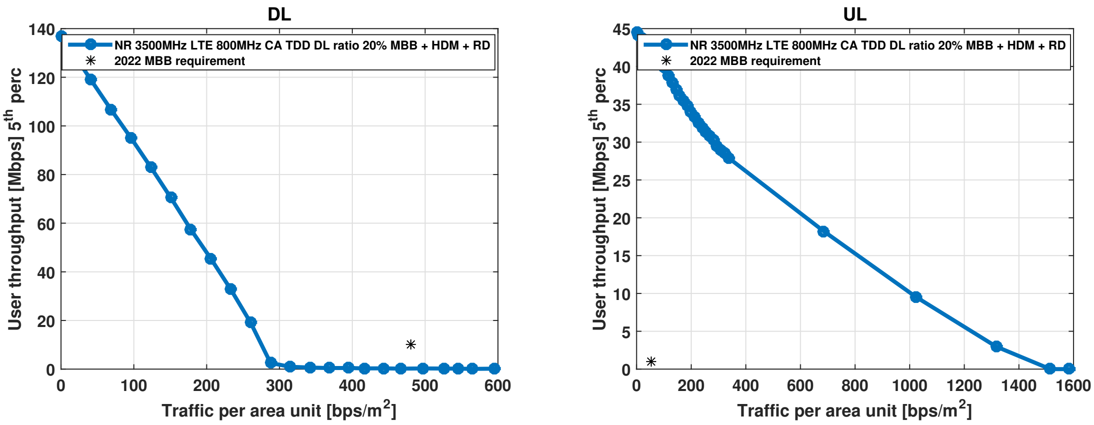

(a) (b)

Figure 44: User throughput as a function of traffic per area unit when using setup G. The HDM vehicle density is set to 10% and the map data size is set to 4 MB/km (a) DL MBB impact (b) UL MBB impact

4.3 Dedicated Carrier Deployment

One possible scenario is to deploy a dedicated carrier for V2N communication. In the following simulations we are excluding the traffic from MBB and look at how the V2N use cases are performing alone.

4.3.1 HDM only

For the first section it is assumed that the carrier dedicates all the spectrum for the HDM use case. For this simulation, NR standalone technology, setup C, is used. As is seen in figure 45, by using the dedicated carrier even the toughest scenario is fulfilled. This is to be compared with figure 33a in section 4.2.3, where the same setup is used, but for a co-channel deployment. As noticed when comparing the figures, using a dedicated carrier enables support for the 4 MB/km scenario.

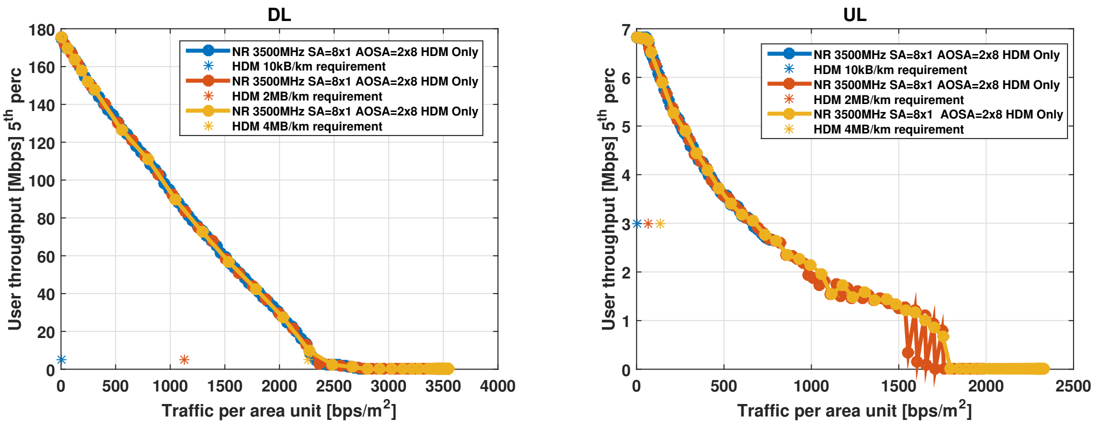

(a) (b)

Figure 45: Showcasing the performance when using a dedicated carrier (no MBB traffic) with setup C. The HDM vehicle density is 10% and the velocity is set to 24 km/h (a) DL (b) UL

4.3.2 HDM and RD only

In similar fashion as the previous section, a carrier dedicated for only HDM and RD traffic is here considered. Based on the findings from when using a co-channel deployment (section 4.2.4), setup G is examined. As seen in figure 46, when using a map data size of 10 kB/km the RD requirement is fulfilled when using a dedicated carrier. This was not the case for the co-channel deployment. Figure 47 illustrates simulation results when changing the map data size to 4 MB/km. The RD requirement can no longer be fulfilled in the DL. A balance of TDD DL ratio is attempted by going from 20% to 30% (i.e setup F). Unfortunately the RD requirement is now not fulfilled in neither the DL nor UL, as made clear in figure 48. A dedicated carrier can thus not solve the scenario of 4 MB/km, 24km/h and 10% HDM cars when using this system configuration.

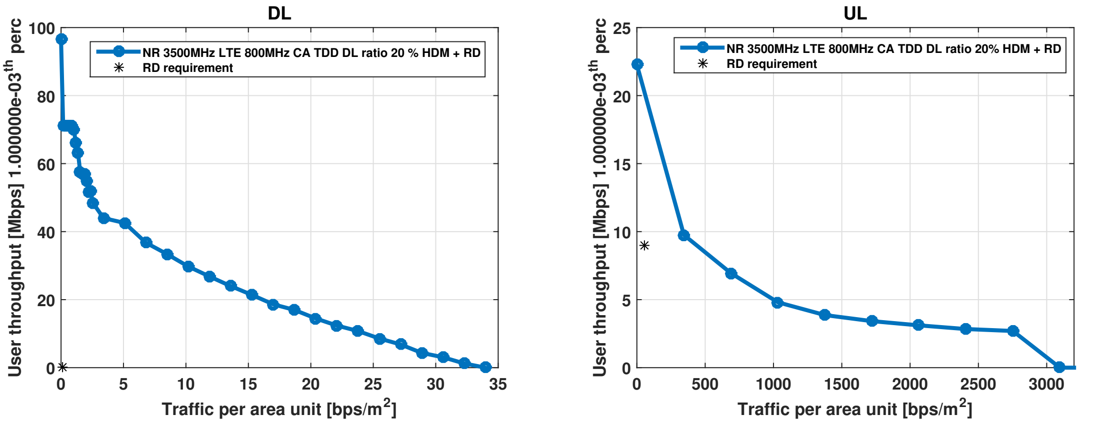

(a) (b)

Figure 46: Showcasing the performance when using a dedicated carrier (no MBB traffic) with setup G. HDM probability is 10% and the map data size is 10 kB/km (a) DL (b) UL

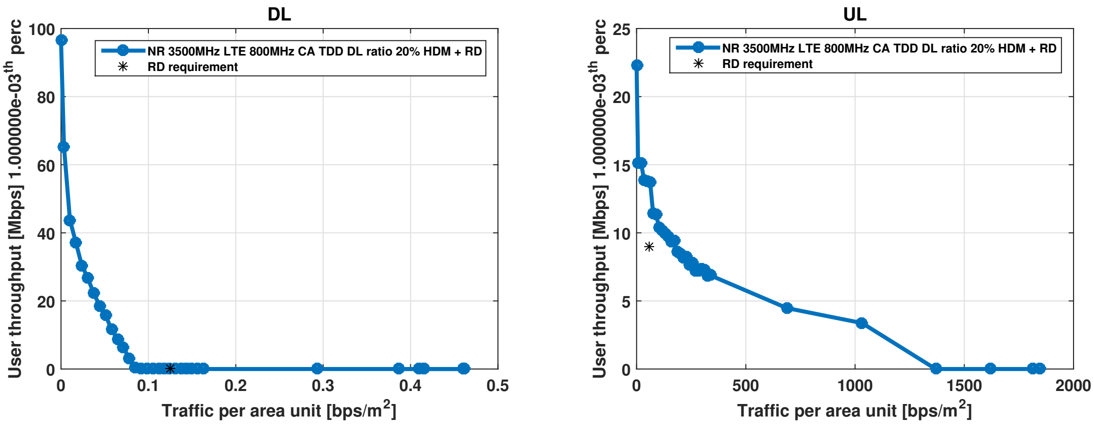

(a) (b)

Figure 47: Showcasing the performance when using a dedicated carrier (no MBB traffic) with setup G. HDM probability is 10% and the map data size is 4 MB/km (a) DL (b) UL

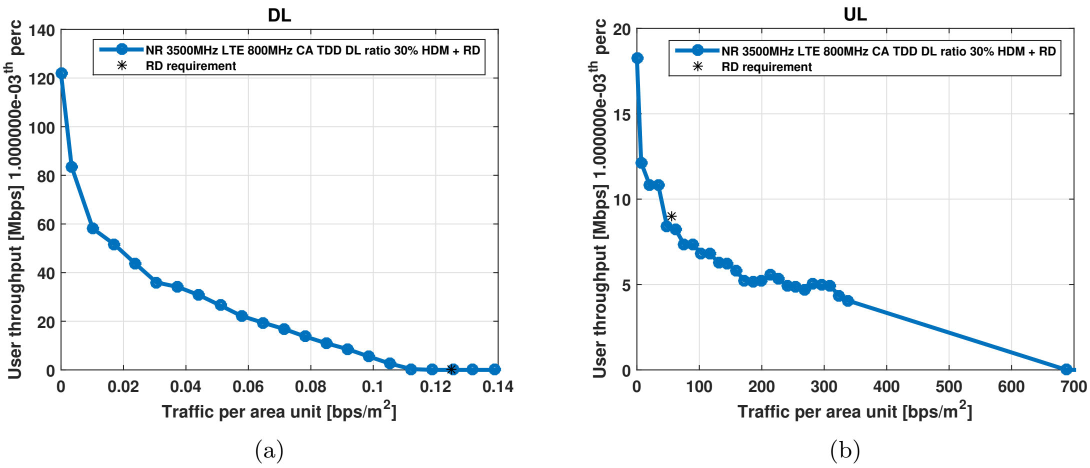

Figure 48: Showcasing the performance when using a dedicated carrier (no MBB traffic) with setup F. HDM probability is 10% and the map data size is 10 kB/km (a) DL (b) UL

4.4 UE Output Power for CA

As made clear in section 2.2, the UL performance analysis is representing an upper-bound. This is due to the fact that the maximum output power is assumed to be doubled, transmitting the same power per band. By reducing the maximal output power per band, and keeping the total output power constant, the lower and upper-bounds can be compared. As is showcased in figure 49, the MBB performance is decreased when using 20dBm in comparison to 23dBm. The true performance curve is contained between these two lines, which indicate that the MBB requirement is fulfilled even when assuming the lower-bound.

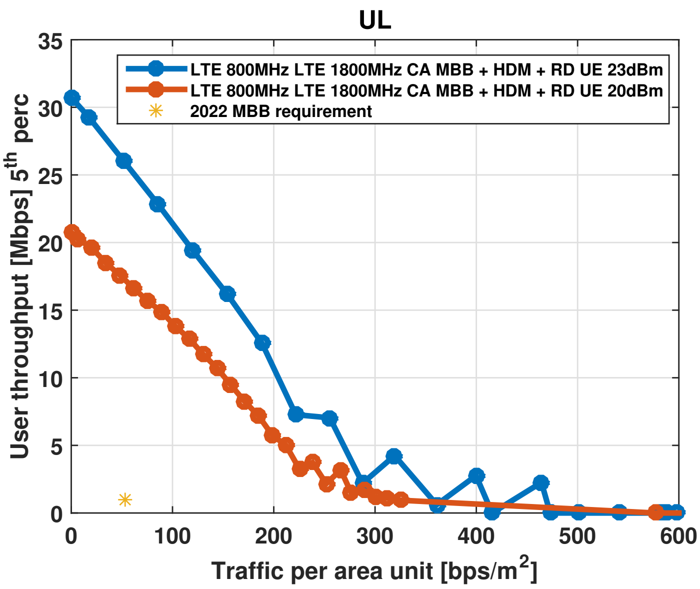

Figure 49: Showing the lower and upper-bound in UL when using CA with setup D

5 Conclusions

Throughout the report three different use cases have been investigated and their impact on the cellular network have been studied. For each use case, performance requirements and traffic demands have been defined and a novel method for generating a road map has been achieved.

In terms of performance results, it can be concluded that the mobile broadband experience for vehicle users will be impacted by transmission of real-time high definition maps and remote driving. Furthermore, a major conclusion is that either carrier aggregation, using LTE technology (40 MHz BW) or LTE-NR interworking (120 MHz BW), is needed in order to fulfill the MBB requirement. It is also noted that in order to satisfy the requirement when experiencing a high car density together with high data traffic from the HDM use case, LTE-NR 120 MHz interworking is required.

When it comes to the performance evaluation of the HDM use case, it is noted that the LTE 40 MHz BW carrier aggregation setup struggles to meet the HDM requirement when the car density is high. Furthermore, it is established that the LTE-NR 120 MHz interworking setup is able to satisfy the requirements for all scenarios considered in this report. Using standalone NR technology also achieves all the requirements, but only when relying on a dedicated V2N carrier (i.e. excluding MBB traffic).

Lastly, it is concluded that the RD use case is profoundly difficult to satisfy when using the configurations considered in this report. Neither the LTE 40 MHz BW CA setup nor LTE-NR 120 MHz BW interworking setup are able to fulfill the RD requirement for the worst-case scenario of high car density (with large probability of RD cars) and high inference from the HDM use case. Furthermore, in order to fully support the non-worst-case scenarios, a lower NR TDD DL ratio is required (which impacts the MBB traffic). Thus, it is concluded that this use case requires either a denser site deployment, a larger bandwidth (120 MHz not enough), or other techniques such as multi-user MIMO.

6 Future Work

It is essential to acknowledge that this study has only scratched the surface of a much bigger research area. Not only are there endless of use cases to explore, but also a vast number of simulation scenarios with an extensive amount of system combinations. I propose that a simulation environment which is able to cover an increasing number of V2N use cases should be constructed. By concatenating use case scenarios, a more accurate performance evaluation of network load would be accomplished.

Furthermore, it would be of interest to research the performance improvement when aggregating more frequency bands than two. In addition to this, support for DC simulation should be implemented to capture a more near-future scenario, as no plan for CA between LTE and NR has yet been announced. Hence, these simulation results might give optimistic results if assumed to represent state-of-the-art technology. Another parameter which should be included in future work is multi-user MIMO. By enabling this communication technique the performance results are expected to change quite drastically. A further suggested implementation is to make the car penetration loss frequency dependant instead of constant. Lastly, I also suggest a broader analysis of site location by sweeping the ISD and thus getting a better understanding on its performance impact.

In closing remarks, it is made evident that not only is the topic of automotive scenarios and V2N communication prominent, but it also carries great depth and with it plenty of research possibilities.

References

[1] Tomtom, "RoadDNA - Robust and Scalable Localization Technology," 2017.

[2] Ericsson, "Ericsson Mobility Report." `http://www.ericsson.com/mobility-report`, June 2017.

[3] 5G-Infrastructure-Association, "5G Automotive Vision." `https://5g-ppp.eu/white-papers/`, October 2015.

[4] 3GPP, "Study on Enhancement of 3GPP Support for 5G V2X Services." `https://portal.3gpp.org/desktopmodules/Specifications/SpecificationDetails.aspx?specificationId=3108`, March 2017.

[5] H. Shimada *et al.*, "Implementation and Evaluation of Local Dynamic Map in Safety Driving Systems," *Journal of Transportation Technologies*, vol. 5, pp. 102–112, 2015.

[6] P. Luoto *et al.*, "System Level Performance Evaluation of LTE-V2X Network," 2016.

[7] P. Popovsk *et al.*, "EU FP7 INFSO-ICT-317669 METIS, D1.1 Scenarios, Requirements and KPIs for 5G Mobile and Wireless System.," 2013.

[8] S. Chen *et al.*, "LTE-V: A TD-LTE-Based V2X Solution for Future Vehicular Network," *IEEE Internet of Things Journal*, vol. 3, pp. 997–1005, 2016.

[9] L. Liu, "Performance Evaluation of Direct Air-to-ground Communication using New Radio (5G)," Master's thesis, Dept. Elect. Eng., KTH, Stockholm, Sweden, 2017.

[10] ITU, "Guidelines for Evaluation of Radio Interface Technologies for IMT-Advanced," technical report, ITU-R M.2135-1, December 2009.

[11] A. Goldsmith, *Wireless Communications*. Cambridge University Press, 2005.

[12] B. P. Lathi, *Modern Digital and Analog Communication Systems. (3 ed.),*. New York: Oxford Univ. Press, 1998.

[13] S. Bernard, "Rayleigh Fading Channels in Mobile Digital Communication Systems Part I: Characterization," *IEEE Communications Magazine*, vol. 35, no. 9, 1997.

[14] Y. Okumura *et al.*, "Field Strength and its Variability in VHF and UHF Land-mobile Radio Service," *Review of the ECL*, no. 16, pp. 825–873, 1968.

[15] M. Hata, "Empirical Formula for Propagation Loss in Land Mobile Radio Service," *IEEE Trans. on Vehicular and Technology VT-29*, no. 16, pp. 317–325, 1980.

[16] M. Iwamura, H. Takahashi, and S. Nagata, "Relay Technology in LTE-Advanced," *NTT Docomo Technical Journal*, vol. 12, no. 2, pp. 29–36, 2010.

[17] 3GPP, "Evolved Universal Terrestrial Radio Access (E-UTRA); Band 41 High Power UE (HPUE)." `https://portal.3gpp.org/desktopmodules/Specifications/SpecificationDetails.aspx?specificationId=2943`, June 2016.

[18] S. C. Jha *et al.*, "Dual Connectivity in LTE Small Cell Networks," *IEEE Globecom Workshops (GC Wkshps)*, 2014. DOI: 10.1109/GLOCOMW.2014.7063597.

[19] D. Warren and C. Dewar, "Understanding 5G: Perspectives on Future Technological Advancements in Mobile," report, GSMA Intelligence, December 2014.

[20] Ericsson, "5G Radio Access," Tech. Rep. Uen 284 23-3204 Rev C, April 2016. `https://www.ericsson.com/assets/local/publications/white-papers/wp-5g.pdf`.

[21] Bundesanstalt für Straßenwesen (BASt) - Federal Highway Research Institute, "Traffic and Accident Data. Summary Statistics - Germany." `http://www.bast.de/EN/Publications/`

Media/Unfallkarten-national-englisch.pdf?__blob=publicationFile, Septermer 2016.

[22] "Taxonomy and Definitions for Terms Related to Driving Automation Systems for On-Road Motor Vehicles," standard, SAE J 3016, January 2014.

[23] European Environment Agency, "Occupancy Rates of Passenger Vehicles." https://www.eea.europa.eu/data-and-maps/indicators/occupancy-rates-of-passenger-vehicles/, April 2016.

[24] A. Shashua and S. Shalev-Shwartz, "Systems and Methods for Identifying Landmarks." US2017/0010120A1, 2017.

[25] J. Levinson, *AUTOMATIC LASER CALIBRATION, MAPPING, AND LOCALIZATION FOR AUTONOMOUS VEHICLES*. PhD thesis, Dept. CS. Eng., Stanford University, Stanford, CA, USA, 2011.

[26] Business Insider Intelligence, "10 million self-driving cars will be on the road by 2020." http://www.businessinsider.com/report-10-million-self-driving-cars-will-be-on-the-road-by-2020-2015-5-6?r=US&IR=T&IR=T, June 2016.

[27] Chris Veness, "Movable Type Scripts." http://www.movable-type.co.uk/scripts/latlong.html, 2017.

[28] FGSV, "Richtlinien für die Anlage von Autobahnen (RAA)," regulation, RAA08, May 2008.

Appendices

A Cord2meter matlab function

```
function dist = cord2meter(lat1,lon1,lat2,lon2)
    R = 6378.137; % Radius of earth in km

    dLat = lat2 * pi / 180 - lat1 * pi / 180;
    dLon = lon2 * pi / 180 - lon1 * pi / 180;
    a = sin(dLat/2) * sin(dLat/2) + ...
    cos(lat1 * pi / 180) * cos(lat2 * pi / 180) * ...
    sin(dLon/2) * sin(dLon/2);
    c = 2 * atan2(sqrt(a), sqrt(1-a));
    d = R * c;
    dist = round(d * 1000); % meters

end
```

B Script for expanding segment elements before interpolation

```
tempCentral = centralLineLon;

uStep = 0;
uStep2 = 1;
newVar = 1;
for k = 1:9-length(centralLineLon)

    if length(tempCentral)>=length(centralLineLon)*2
        insert = centralLineLon(newVar)+2;
        tempCentral = [tempCentral(1:newVar+uStep2)' insert tempCentral(newVar+uStep2+1:end)']';
        uStep2 = uStep2 + 2;
        newVar = newVar + 1;
    else

        insert = centralLineLon(k)+1;
        tempCentral = [tempCentral(1:k+uStep)' insert tempCentral(k+uStep+1:end)']';
        uStep = uStep + 1;

    end


end

centralLineLon = tempCentral;
```

C Square creation algorithm

```
%map is the road matrix containing ones and zeros
in = 3; %representing bin inside motorway
out = 4; %representing bin outside motorway

t_col = floor(size(map,2)/2);
t_row = floor(size(map,1)/2);
t = floor(t_col * t_row); %the number of comparisons we will make

map_temp = zeros(size(map,1),size(map,2));

for i = 1:2:t_row*2
    for j = 1:2:t_col*2

        if any(any(map(i:i+1,j:j+1) == 1)) %we look if any of the selected elements
    contain 1, otherwise we have only 0's
            if length(find(map(i:i+1,j:j+1) == 1)) >= length(find(map(i:i+1,j:j+1)
    == 0)) %If we have 2 or more 1's we set it to 1
                map_temp(i,j) = in;
            else
                map_temp(i,j) = out;
            end
        else
            map_temp(i,j) = out;
        end

    end
end

map = map_temp;
```

D Coverage plots for ISD 4 km

Figures 50 and 51 showcase coverage maps for setup D and E, when having an ISD of 4 km. As made clear from the figures, setup E performs significantly better than setup D when it comes to the DL. However, when comparing the cell-edge and average throughput for the UL, the setups perform the same.

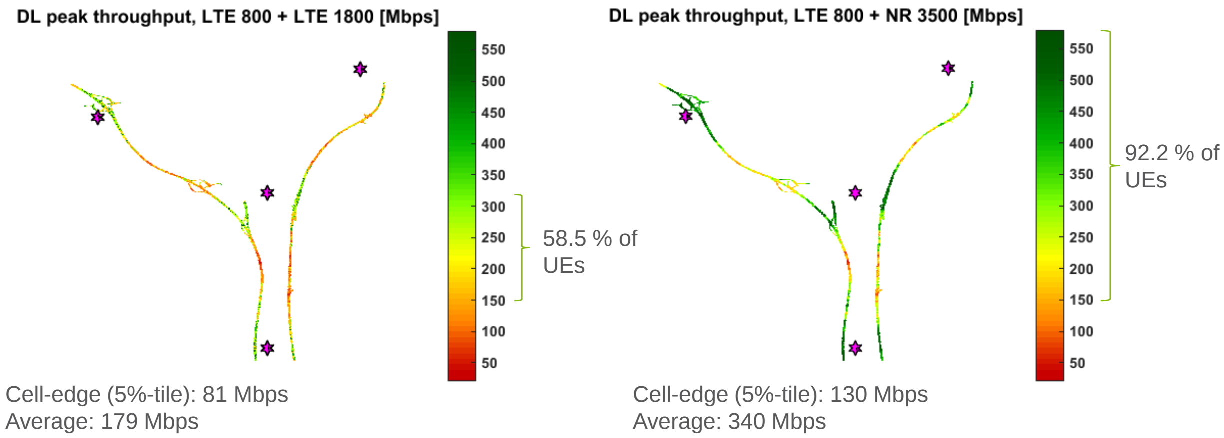

Figure 50: Coverage map: DL peak throughput for setup D and E. Average and cell-edge throughput is shown for each setup, as well as the percentage of UEs which experience 150 Mbps or more. The ISD is set to 4 km

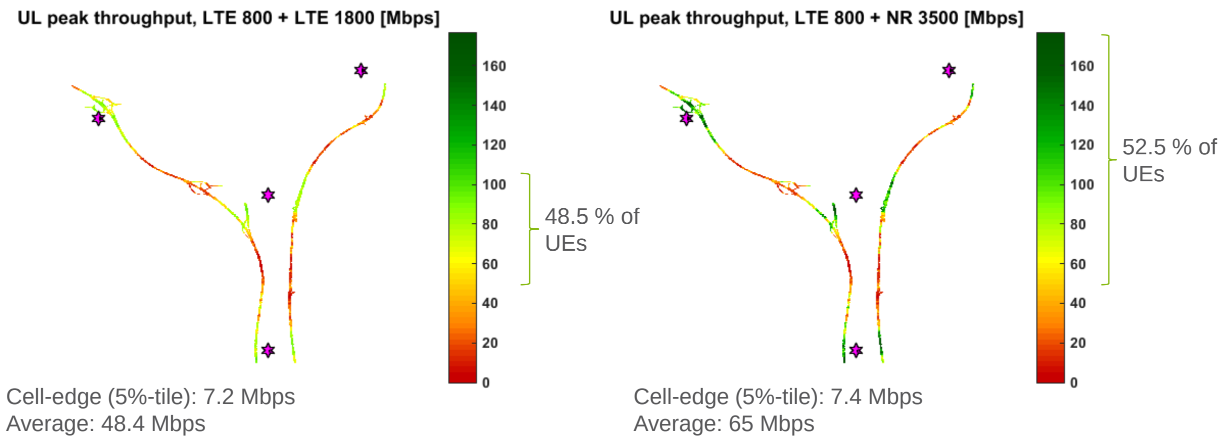

Figure 51: Coverage map: UL peak throughput for setup D and E. Average and cell-edge throughput is shown for each setup, as well as the percentage of UEs which experience 50 Mbps or more. The ISD is set to 4 km

E Summary of results: MBB performance (v fixed to 24 km/h)

Figure 52 illustrates a summary of results for the MBB performance evaluation. As made evident from the figure, CA technology is required in order to satisfy the worst-case scenario.

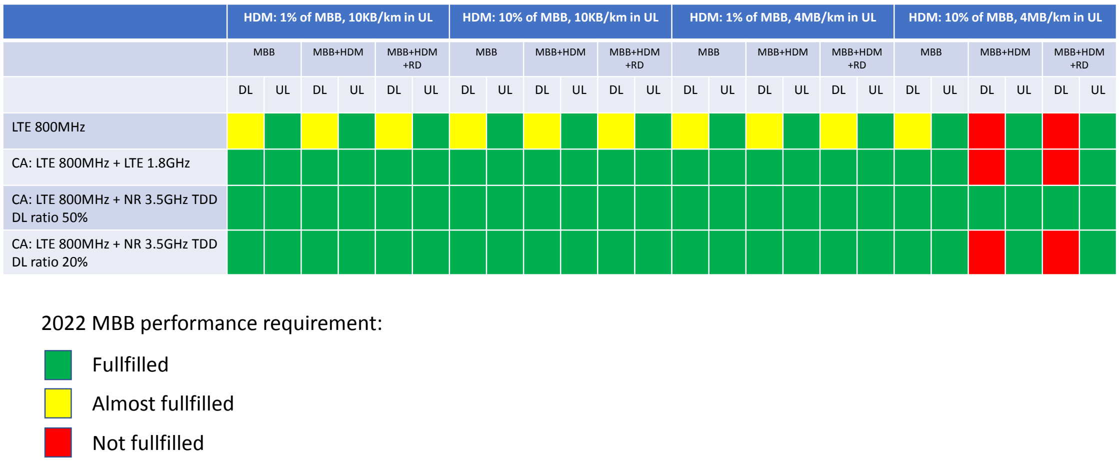

Figure 52: Table of results for MBB performance

F Summary of results: HDM performance (all velocities)

Figure 53 illustrates a summary of results for the HDM performance evaluation. As made evident from the figure, setup D struggles when having high car density. It is also shown that setup E is able to support all scenarios. If impact on MBB traffic should be avoided, setup C is able support all scenarios when deployed on a dedicate V2N carrier.

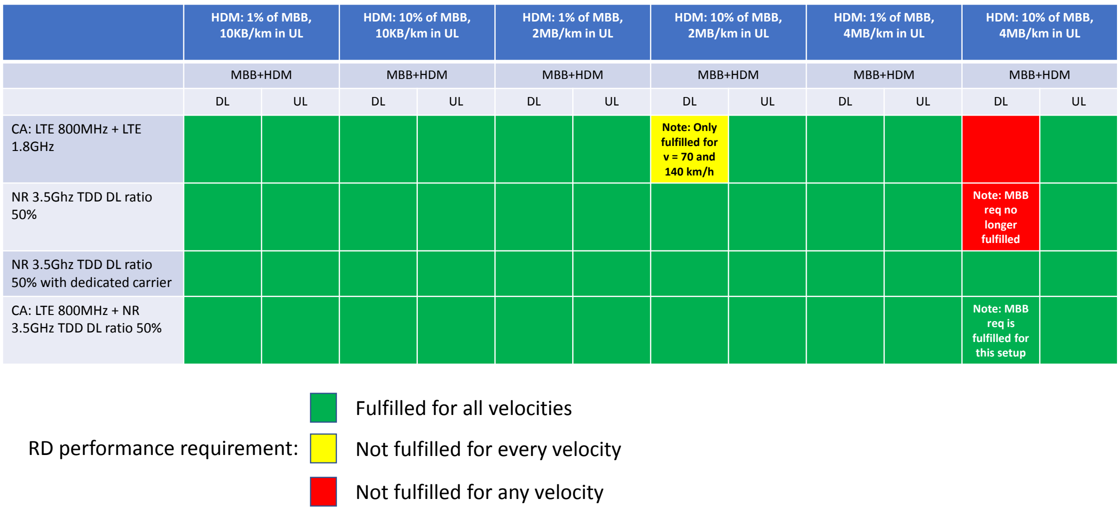

Figure 53: Table of results for HDM performance

G Summary of results: RD performance (v fixed to 24 km/h)

Figure 54 illustrates a summary of results for the RD performance evaluation. As made evident from the figure, both setup D and E struggle with the high car density scenarios. It is also shown that more scenarios are fulfilled when lowering the TDD DL ratio (i.e setup F or G). None of the setups are able to satisfy the requirements for the worst-case traffic scenarios.

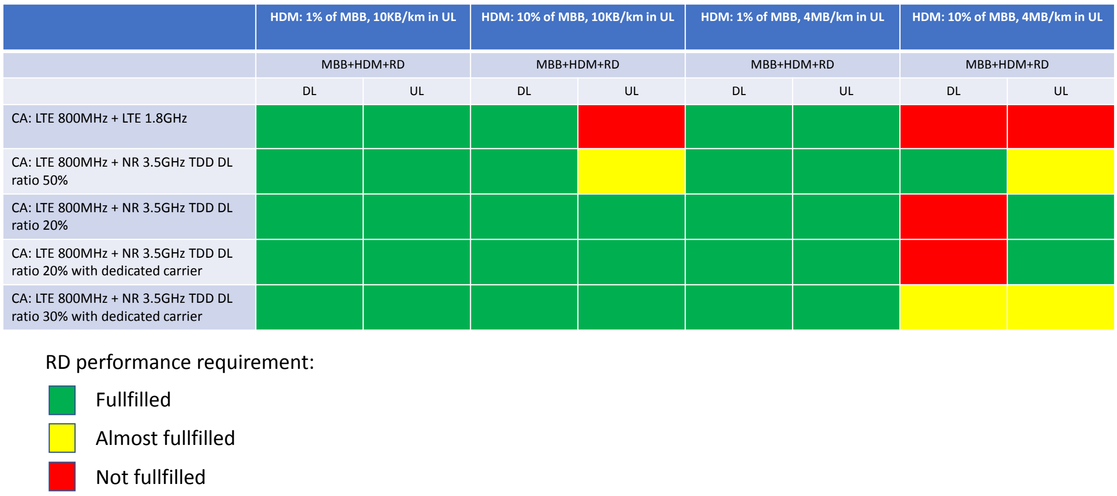

Figure 54: Table of results for RD performance